nature plants

Article

https://doi.org/10.1038/s41477-025-02089-4

Arbuscular mycorrhizal association regulates global root–seed coordination

Received: 28 January 2025

Accepted: 25 July 2025

Published online: 19 August 2025

Check for updates

Qingpei Yang[1], Binglin Guo[1], Mingzhen Lu[2], Yanjie Liu[3], Paul Kardol[4,5], Peter B. Reich[6,7,8], Richard D. Bardgett[9], Johannes H. C. Cornelissen[10], Nathan J. B. Kraft[11], Sandra Díaz[12,13], Ian J. Wright[8,14], Nianpeng He[15], J. Aaron Hogan[16], Yuxin Pei[1], Qinwen Han[1], Zhenjiang Li[1], Zheng Wang[17], Wanqin Yang[18], Junxiang Ding[19], Zhongling Yang[20], Huifang Wu[1], Carlos P. Carmona[21], Oscar J. Valverde-Barrantes[22], Dezhu Li[23,24], Jie Cai[24], Hui Zeng[25], Yue Zhang[1], Weizheng Ren[1], Yong Zhao[1], Xitian Yang[1], Guoqiang Fan[1], Junjian Wang[26,27] ✉, Guoyong Li[20] ✉ & Deliang Kong[1] ✉

Terrestrial plants exhibit immense variation in their form and function among species. Coordination between resource acquisition by roots and reproduction through seeds could promote the fitness of plant populations. How root and seed traits covary has remained unclear until our analysis of the largest-ever compiled joint global dataset of root traits and seed mass. Here we demonstrate that seed mass and seed phosphorus mass scale positively with root diameter in arbuscular mycorrhizal (AM) plants, depending on variation in root cortical thickness instead of root vessel size. These findings suggest a dual role of AM association in phosphorus uptake and pathogen resistance which drives the global root–seed coordination, instead of initially expected resource transport via root vessels as the main driver. In contrast, we found no relationship between root traits and seed mass in ectomycorrhizal plants. Overall, our study reveals coordination between roots and seeds in AM plants, which is probably regulated by root–mycorrhizal symbiosis, and may be crucial in shaping global plant diversity and species distributions.

Terrestrial plants vary greatly in their form and function to cope with heterogeneous natural environments, which contributes fundamentally to Earth's biodiversity[1–6]. Substantial global variation in plant form and function has been shown to be captured by a two-dimensional (2D) space defined by aboveground plant traits critical to growth, survival and reproduction, including leaf, stem and seed traits[1]. One dimension is related to plant size, consistent with Corner's rules[7], which state that larger plants are more likely to have larger leaves, stems and seeds because they usually bear larger meristems[8–10]. The other dimension coincides with the leaf economics spectrum[3], representing a trade-off between the capacity of rapid carbon acquisition in leaves and their investment cost[3,8].

Recently, studies have demonstrated that root traits also vary in a 2D trait space[2,6,11]. The first dimension represents a collaboration gradient for mycorrhizal symbiosis, ranging from 'do-it-yourself' resource acquisition characterized by finer absorptive roots, to 'outsourcing' of resource acquisition through mycorrhizal fungi associated with thicker absorptive roots and higher levels of mycorrhizal colonization[6]. The second dimension reflects a resource conservation gradient, highlighting a trade-off between acquisitive (high root nitrogen concentration) and conservative strategies (high root tissue density). This gradient has been suggested to align with the plant fast-slow economics spectrum[6,7], although the generality of coordination among plant size, economic spectrum and mycorrhizal collaboration is still debated[2,12]. Over evolutionary time, roots in coordination with aboveground plant organs have enabled vascular plants to adapt to heterogeneous environments in diverse ways[6,12,13]. For example, traits that represent the

A full list of affiliations appears at the end of the paper. ✉e-mail: wangjj@sustech.edu.cn; ligy535@henu.edu.cn; deliangkong1999@126.com

https://doi.org/10.1038/s41477-025-02089-4

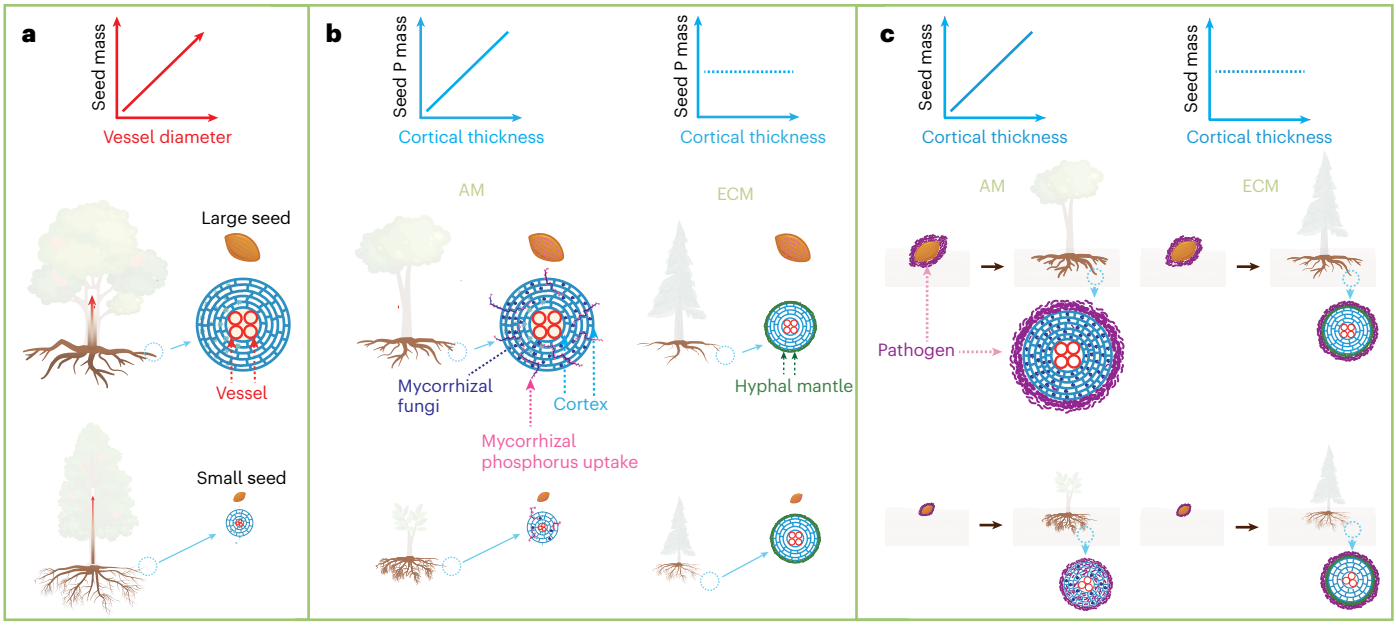

Fig. 1 | Three hypotheses regarding the relationships between roots and seeds. a, Resource transport hypothesis: larger seeds are associated with thicker root vessels, enhancing nutrient transport efficiency to support seed growth. **b**, Mycorrhizal P uptake hypothesis: the development of larger seeds with greater P demand (that is, from higher seed P mass) entails thicker root cortices which usually have more AM colonization, and hence more P uptake (solid pink filled circles) by AM fungi. In contrast, there is no such correlation in ECM plant species. **c**, Pathogen resistance hypothesis: predicts a positive relationship between root cortical thickness and seed mass. On the left half of **c**, larger seeds of AM plant species (both woody and non-woody) are predicted to develop thicker root cortices, which attract mycorrhizal fungi to help defend roots against soil pathogens. This leads to a positive correlation between root cortical thickness and seed mass in AM plants. In contrast, the right half of **c** predicts that ECM plant species, whose roots are protected by an ECM hyphal sheath, will show no correlation between root cortical thickness and seed mass.

resource conservation dimension in the root economics space, such as root tissue density and root nitrogen concentration, often correlate with traits from the leaf economics spectrum, such as leaf nitrogen concentration and leaf mass per area[12]. Notably, these economics traits vary independently from the size dimensions of the leaves, stems and seeds[1,13,14].

While our understanding of the coordination between roots and aboveground organs has advanced in recent years[2,6,12,13], it remains uncertain whether, and if so, how and why roots are coordinated with seeds. More than two-thirds of the world's plant species rely on seeds for reproduction, population maintenance and establishment in new habitats[15,16]. Seed mass is of particular importance for species' dispersal, seedling survival and plant–animal interactions[15,17,18]. Generally, larger seeds are dispersed by larger animals[15,17] and produce seedlings with larger pathogen resistance and higher survival rates[19,20]. Remarkably, terrestrial plants display a range of 13 orders of magnitude in seed mass[1,15,16]. Examining how roots and seeds are coordinated is therefore a critical step toward fully understanding the global variation in plant form and function that supports biodiversity on Earth.

Theoretically, roots and seeds are interconnected during at least two stages of the plant's life cycle. First, during the reproductive stage, seed formation depends on water, carbon and mineral nutrients transported from vegetative organs, that is, roots, stems and leaves[21]. Therefore, seed size could be coupled with vessel size that is responsible for matter transport efficiency during this stage. Such a relationship is also suggested by Corner's rules. Alternatively, larger seeds have a greater demand of phosphorus (P) to support more cell division as larger seeds develop. This will generate selective pressure for building thicker absorptive roots in larger-seeded plants to deploy more cortex-residing mycorrhizal fungi for more P acquisition[22]. Second, in the recruitment stage, the carbon and nutrients needed to establish initial vegetative organs (including the first roots, stems and leaves) are derived primarily from the seed itself[21]. Larger seeds, which store more carbon and nutrients, face a higher risk of pathogen infection[23]. In this context, producing thicker absorptive roots which are often enriched with mycorrhizal fungi that colonize the cortex[6,24] could help enhance pathogen resistance[25]. While some studies have reported a positive correlation between root diameter and seed size, they have focused on a limited number of species (primarily temperate non-woody species, possibly due to the difficulty of getting detailed root information for woody plants) and were based on restricted geographical sampling[11,20,26–28]. Consequently, the global coordination between roots and seeds remains unclear. Here we aimed to uncover this global coordination between roots and seeds, especially in terrestrial woody plants, and to elucidate the underlying mechanism.

Three working hypotheses

We propose three alternative hypotheses to explaining the root–seed relationship (Fig. 1):

(1) The resource transport hypothesis. Based on Corner's rules[7] and the metabolic theory of ecology[29,30], we hypothesized that plants with larger seeds have higher metabolic demand, requiring a larger-vessel root vascular system to support nutrient and water transport, overall higher carbon assimilation and seed growth. Generally, soil nutrients are acquired by roots and mycorrhizal fungi. Nutrients then move into root vessels before being transported to seeds. If seed size is limited by nutrient transport via vessels rather than by nutrient acquisition, we predicted a positive correlation of seed size with root vessel diameter and root diameter, given that roots with larger diameters generally have wider vessels[24,31] (Fig. 1a).

(2) Mycorrhizal P uptake hypothesis. If seed size is primarily limited by nutrient acquisition especially P, we expect that plants with thicker absorptive roots, and hence more arbuscular mycorrhizal (AM) colonization, would be better able to meet the high P

https://doi.org/10.1038/s41477-025-02089-4

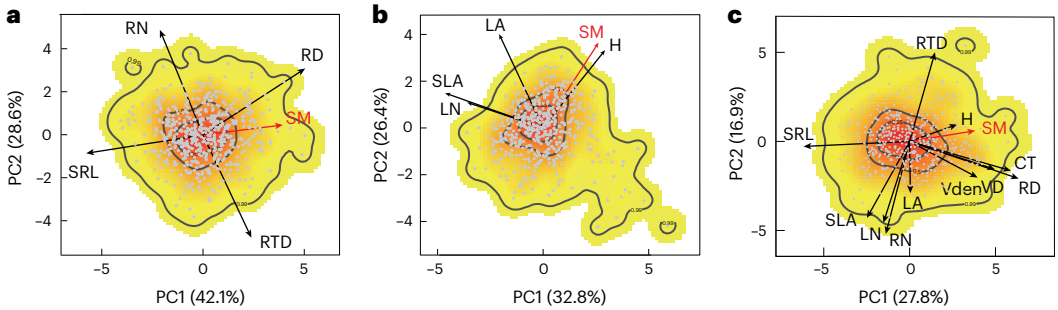

Fig. 2 | Integration of seed mass within the above- and belowground plant trait space. Analyses were performed using our field-measured trait data: **a**, Seed mass and the four traits associated with the previously described 2D root economics space (SRL, RTD, RN and RD). **b**, Seed mass, two traits associated with the plant size dimension (LA and H) and two traits associated with the leaf economics spectrum (SLA and LN). **c**, All traits from **a** and **b**, combined with root anatomical traits (CT, VD and VDen). Colour gradients indicate species occurrence probability within the trait space, with red indicating high occurrence and yellow indicating low occurrence. Contour lines correspond to the 0.25, 0.50 and 0.99 quantiles. Grey filled circles represent the field-measured plant species in this study. Traits included in each dimension are: leaf economics spectrum (specific leaf area, SLA; leaf nitrogen concentration, LN); plant size (seed mass, SM; leaf area, LA; mature plant height, H); root economics space (root diameter, RD; specific root length, SRL; root tissue density, RTD; root nitrogen concentration, RN); and root anatomical traits (cortical thickness, CT; vessel diameter, VD; vessel density, VDen).

demand for producing larger seeds. Therefore, a positive correlation would be expected between root cortical thickness and seed P mass (where seed P mass = seed mass × seed P concentration). In contrast, ectomycorrhizal (ECM) roots, where there is no or very little contact between the root cortex and the soil solution (as the ECM fungal mantle completely or largely covers the roots), do not select for cortical area, ultimately resulting in lack of the above correlation (Fig. 1b).

(3) The pathogen resistance hypothesis. Although large seeds (usually with more internal nutrient reserves) can disperse over long distances, many still fall near the parent plant[32–34], where soil pathogens to which a species is susceptible are likely to be more abundant. This phenomenon is known as the Janzen–Connell effect[35,36]. A prerequisite for the pathogen resistance hypothesis (but also for the mycorrhizal P uptake mechanism) is that there is a differential relationship between seed size and cortical thickness for AM and ECM plants. Specifically, in AM plants, larger seeds tend to be associated with thicker absorptive roots with thicker cortices to allow room for greater mycorrhizal colonization[36,37] and enhanced pathogen protection[25,37], while no such relationship is expected in ECM plants because their absorptive roots are already encased in protective mycelial sheaths against pathogens[38,39] (Fig. 1c).

Results and discussion

A global dataset on roots and seeds

To test our hypotheses, we collected samples of roots, stems, leaves and seeds from 660 woody plant species across 11 forest types in China, spanning climates from tropical to temperate regions (Extended Data Table 1). We measured seed traits including dry mass, length and width, and examined root anatomical traits such as cortical thickness, stele radius, vessel diameter and vessel density, capturing key aspects of root morphology variation, specifically the mycorrhizal collaboration dimension. In addition, we analysed two classic traits within the root conservation dimension: root tissue density and root nitrogen concentration. Leaf traits, including nitrogen concentration and specific leaf area, were assessed to examine the leaf economics spectrum[1,3,4], along with mature plant height, as these traits are associated with seed construction and dispersal[1,4].

To explore the global relationship between roots and seeds, we also compiled data from the Global Root Traits (GRooT) database[40] and other literature, incorporating 620 additional species with both root and seed traits data. Totally, this global dataset (our field-measured data plus those from the GRooT database and literature) includes 239 plant families and spans two major mycorrhizal types (1,023 AM plants and 142 ECM plants), three growth forms (331 herbs, 329 shrubs and 636 trees) and diverse climatic zones (380 tropical plants, 450 subtropical plants and 467 temperate plants) (Extended Data Fig. 1). This comprehensive dataset allowed us to investigate the universality of root–seed relationships.

The global root–seed coordination

Before analysing the root–seed relationship using field-measured data, we first explored the dimensions of the trait variation in roots, leaves and seeds. This step was necessary because if trait variations in those organs are different from those well documented in previous studies[1,6,14], the root–seed relationship derived from the field-measured data might represent a specific case rather than a general pattern. The results of principal component analysis (PCA) show that absorptive root traits align with the two orthogonal dimensions: mycorrhizal collaboration gradient and the conservation gradient[2,6] (Fig. 2a). In contrast, variations in aboveground plant traits (Fig. 2b), consistent with Corner's rules, align with the established axes of the leaf economics spectrum[3] and plant size dimensions including mature plant height and seed mass[1] (Fig. 2c). We also observed coordinated variation of the conservation spectrum between above- and belowground traits, for example, the closely aligned ordination vectors for leaf and root N concentration (Fig. 2c).

We also found that, in both our field-measured trait study (Extended Data Fig. 2a,b) and in the global dataset (Fig. 3a), seed mass is significantly and positively correlated with the mycorrhizal collaboration gradient, particularly root diameter, which represents the volume of the intraradical habitat for fungal partners[6]. However, seed mass shows no relationship with the conservation dimension of roots (Fig. 2a). This positive relationship between root diameter and seed mass holds consistently across different climatic zones (tropical, subtropical and temperate) and woody species (trees and shrubs), with the effect being pronounced in AM plant species (Extended Data Figs. 3a,d and 4a,d,g) and absent in ECM plant species. By integrating our new data with existing literature, we demonstrate that the root diameter–seed mass relationship is robust across plant growth forms, including woody and non-woody species (Extended Data Fig. 5). Moreover, this relationship remains consistent even after accounting for plant phylogeny (Extended Data Fig. 6).

Mechanisms of root–seed coordination

We explored potential mechanisms underlying the observed relationships between roots and seeds (Fig. 1). We found a relatively weak or no correlation between root vessel diameter and seed mass using

https://doi.org/10.1038/s41477-025-02089-4

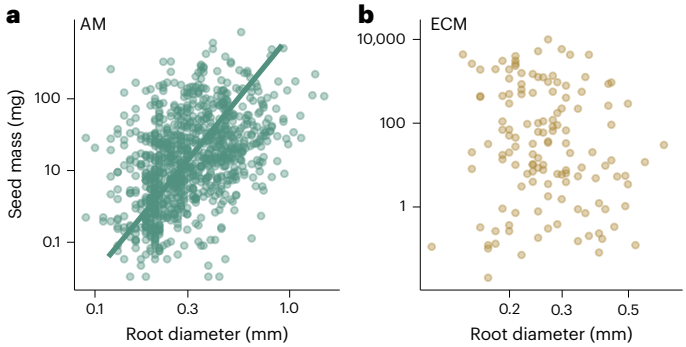

Fig. 3 | Global relationship between root diameter and seed mass. **a**,**b**, Analyses were performed for AM (**a**) and ECM plant species (**b**) using combined field-measured data and literature data. Global AM data show a significant positive correlation (**a**): green filled circles; regression equation: $\log_{10}(y) = 6.23 \log_{10}(x) + 4.43$, $r = 0.45$, $P = 2.2 \times 10^{-16}$, $n = 983$. Both regressions were performed using the standardized major axis (SMA) regression. The scaling exponent for the AM plant species is 6.23 (95% confidence interval (CI) = 5.89–6.59) ($P = 1.32 \times 10^{-6}$; see Methods). In contrast, no significant correlation was found for ECM plant species (**b**): tan filled circles; $r = 0.11$, $P = 0.20$, $n = 131$. Significance was tested using a two-sided t-test. All data are plotted on logarithmic scales ($\log_{10}$) for both axes, with each point representing a single plant species.

field-measured data (Fig. 4a and Extended Data Fig. 3c). Conditional correlation analyses considering the significant relationship between cortical thickness and vessel diameter ($r = 0.52$, $P < 0.01$) showed no correlation between vessel diameter and seed mass ($r = 0.03$, $P < 0.54$) in AM plants. Remarkably, this correlation was also absent within each mycorrhizal type (Extended Data Figs. 3f and 4c,f,i), climatic zone (Extended Data Fig. 4c,f,i) and among tree and shrub species (Extended Data Fig. 3c,f). This suggests that the positive relationship between root vessel diameter and seed mass, as expected by the resource transport hypothesis, or the widely recognized Corner's rules, cannot fully explain the observed positive relationship between root diameter and seed mass.

Although plant height was positively correlated with seed mass ($r = 0.32$; Extended Data Fig. 6), consistent with the empirical Corner's rules, its weak relationship with root vessel diameter ($r = 0.17$; Extended Data Fig. 6) probably limits the indirect pathway by which vessel traits might influence seed size. These findings may explain why the resource transport hypothesis was not supported. Indeed, the weak correlation between plant height and root vessel diameter warrants further investigation.

In contrast to the root vessel diameter–seed mass relationship, we found a stronger positive correlation between root cortical thickness and seed mass, with a significant correlation in AM plants (green filled circles in Fig. 4b) but no such correlation in ECM plants (green open circles in Fig. 4b). Conditional correlation analysis further confirmed the positive correlation between cortical thickness and seed mass ($r = 0.24$, $P < 0.01$) in AM plants. This root cortex–seed relationship was consistent within each growth form (trees and shrubs) (Extended Data Fig. 3b,e) and climatic zone (tropical and subtropical) (Extended Data Fig. 4b,e,h) in AM plants, while it was absent in ECM plants.

The lack of a significant relationship between vessel diameter and seed mass in ECM plant species further challenges the universal applicability of Corner's rules. In AM plants, thicker cortices are closely related to greater mycorrhizal colonization by providing more intraradical space for fungi symbiosis[6,41]. These AM fungi could enhance phosphorus uptake for larger seed production. Consistent with the expectation of the mycorrhizal P uptake hypothesis, we observed a positive correlation between cortical thickness and seed phosphorus mass ($r = 0.33$, $P < 0.05$) in AM plants and no correlation ($r = 0.001$, $P = 0.88$) in ECM plants. This suggests that the nutritional function of mycorrhizal association, particularly for commonly limiting nutrients such as P, potentially explains the root–seed relationship.

Since our field-measured data (Fig. 4 and Extended Data Fig. 2a,c) were from mature plants and the pathogen resistance hypothesis was originally based on seedling roots[21], we also analysed both mature and seedling roots for the same species, using field samples and literature data. This follow-up analysis showed a strong positive correlation in absorptive root diameter between the mature plants and their respective seedlings (Extended Data Fig. 7), indicating trait consistency over ontogeny. Several lines of evidence also support the pathogen resistance hypothesis and mycorrhizal P uptake hypothesis, which suggests that resistance to soil-borne pathogens together with P uptake by symbiotic mycorrhizal fungi in root cortex may also regulate the root–seed relationship.

First, AM plants, particularly obligate AM species compared with non-mycorrhizal (NM) ones, tend to produce large seeds[19,42,43]. These large seeds give rise to absorptive roots with larger diameters, which attract and sustain more mycorrhizal hyphae; the hyphae, in turn, allow the plants to acquire more P and help fend off soil pathogens[19,25] by secreting antagonistic compounds, enhancing immunity of host roots (even leaves[37]) and/or competing for photosynthate or infection sites in cortical cells[44].

Second, previous studies[36,45,46], along with our integrated analysis, indicate that tropical and subtropical plant species potentially experience greater pathogen pressure than species in temperate regions. The higher levels of mycorrhizal colonization observed in tropical and subtropical roots, as compared with temperate ones (Extended Data Fig. 8a), may be a result of this geographic pattern of soil pathogens. The greater pathogen presence in more moist and warmer climatic zones can, in turn, select for thicker root diameter and root cortex in these regions[31], providing enhanced pathogen resistance probably through the above mechanisms by accommodating more mycorrhizal fungi within the cortex[25]. Moreover, (sub-)tropical ecosystems are well known to experience more prominent P limitation than temperate ecosystems[47]. Consequently, higher mycorrhizal colonization in thicker absorptive roots of (sub-)tropical plants could help meet the elevated P demands associated with producing larger seeds. These phenomena may explain the significant positive correlation between seed mass and both root diameter and cortical thickness (Figs. 3 and 4a).

Third, we note an increasing trend of soil fungal pathogen richness (potentially pathogen combinations or pathogenicity per tree

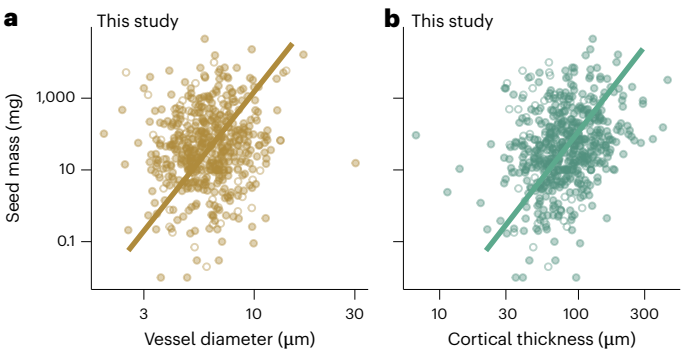

Fig. 4 | Relationships between root anatomical traits and seed mass. The analyses were performed using our field-measured data. **a**,**b**, For AM plant species, seed mass is positively correlated with both vessel diameter (**a**, tan filled circles, $\log_{10}(y) = 7.34 \log_{10}(x) - 4.14$, $r = 0.16$, $P = 1.45 \times 10^{-12}$, 95% CI = 6.71–8.04, $n = 458$) and root cortical thickness (**b**, green filled circles, $\log_{10}(y) = 4.81 \log_{10}(x) - 7.60$, $r = 0.33$, $P = 0.002$, 95% CI = 4.43–5.23, $n = 488$). Both regressions were performed using SMA regression. In contrast, no correlation was observed for ECM plant species (**a**, tan open circles, $r = 0.04$, $P = 0.77$, $n = 71$; **b**, green open circles, $r = 0.06$, $P = 0.62$, $n = 78$; regression lines not shown). Significance was tested using a two-sided t-test. Data are plotted on logarithmic scales ($\log_{10}$) for both axes, with each point representing a single plant species.

https://doi.org/10.1038/s41477-025-02089-4

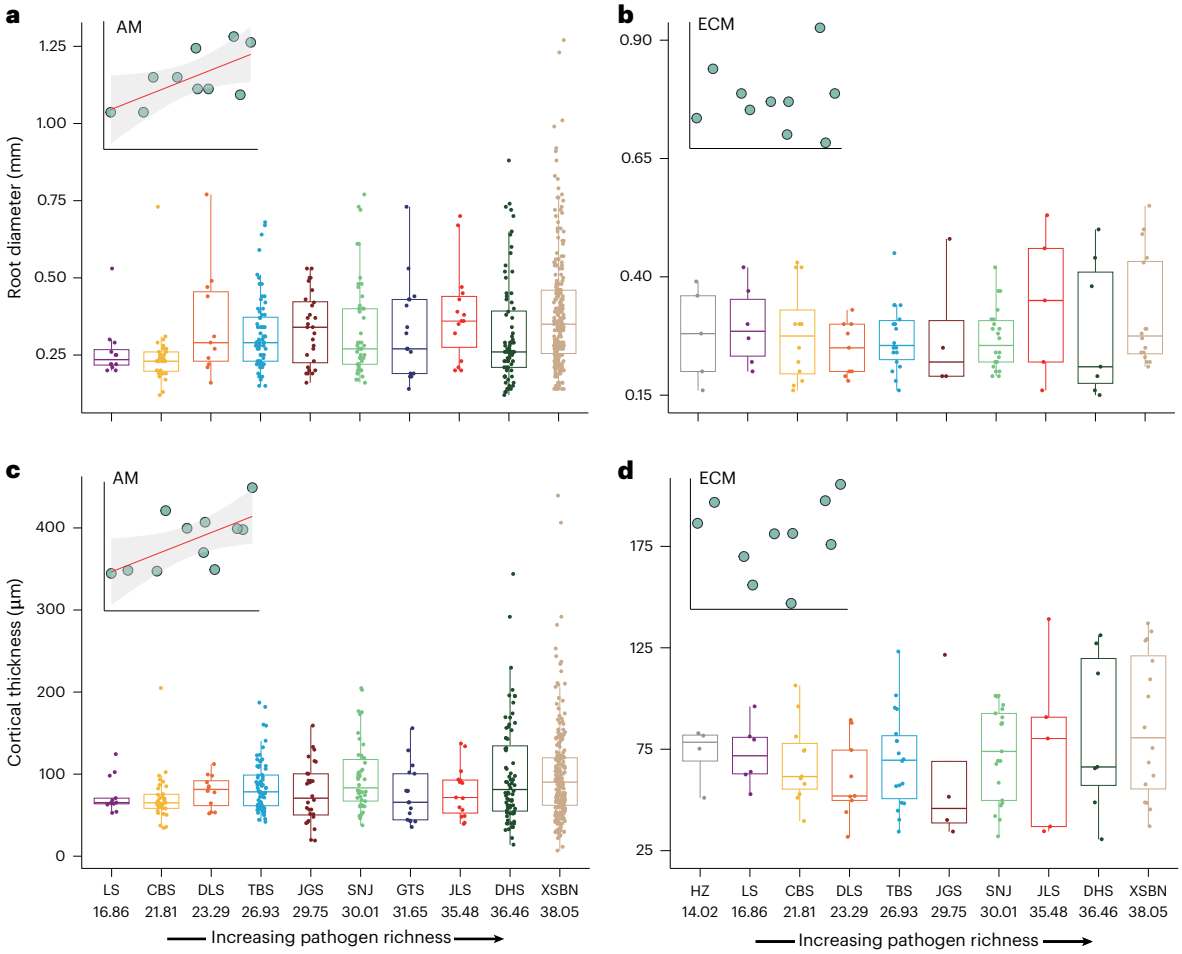

Fig. 5 | Relationships between soil pathogen richness and root traits. Sampling sites in temperate forests include Huzhong (HZ), Liangshui (LS), Changbai Mountain (CBS), Dongling Mountain (DLS) and Taibai Mountain (TBS); subtropical sampling sites include Jigong Mountain (JGS), Shennongjia (SNJ), Gutian Mountain (GTS), Jiulian Mountain (JLS) and Dinghu Mountain (DHS); and tropical species were sampled in Xishuangbanna (XSBN) (see Extended Data Table 1 for details of these sites). **a**–**d**, Boxplots of root diameter (**a**,**b**) ($n = 535$, $n = 104$) and cortical thickness (**c**,**d**) ($n = 535$, $n = 101$) for AM (**a**,**c**) and ECM (**b**,**d**) plant species. For each plot, the sites are arranged in order of increasing soil fungal pathogen richness, with corresponding number of OTUs (obtained by soil fungal sequencing) indicated below each sampling site. Pearson correlation indicates a positive correlation between soil fungal pathogen richness and both root diameter and cortical thickness in AM plant species (inset in **a**, $y = 0.005x + 0.16$, $r = 0.66$, $P = 0.04$; inset in **c**, $y = 0.005x + 0.16$, $r = 0.63$, $P = 0.03$). Shaded areas indicate 95% CIs of the regression lines. In contrast, no significant correlations were observed for ECM plant species (inset in **b**, $r = 0.04$, $P = 0.91$; inset in **d**, $r = 0.14$, $P = 0.69$). Significance was tested using a two-sided t-test. Insets: median values for root diameter and cortical thickness in each sampling site. Soil fungal pathogen richness data were sourced from literature reporting soil fungal pathogen patterns across forest sites in China[46], similar to our sampling sites. Boxplots indicate the median value (solid line), 25th and 75th percentiles (box) and the data range (whiskers).

species) from tropical to cold temperate regions in China[46] (Fig. 5 and Extended Data Fig. 8b–e). Alongside our root anatomical data, we further found strong positive correlations between root diameter, cortical thickness and soil fungal pathogen richness in AM plants (Fig. 5a,c and Extended Data Figs. 8b,d), but not in ECM plants (Fig. 5b,d and Extended Data Fig. 8c,e). Therefore, the significant association between seed mass and the mycorrhizal collaboration dimension of the roots, particularly their role in pathogen defence, probably explains the independence of this dimension from the resource acquisitive-conservative strategy gradient in the previously described root economics space[6]. This relationship provides a novel perspective—well supported by substantial empirical evidence—on the origins of the 2D root economics space[5,48], and offers an interesting expansion on the relationship between chemical protection in roots and potential pathogen pressure[48].

Our results further show no significant correlation of root diameter and seed mass with family divergence time, a proxy of evolutionary age (Fig. 6a,b). This suggests that the environmental selection (for example, increasing pathogen load and/or P limitation in habitats where thick-root species often grow) for this adaptive trait syndrome (that is, thick absorptive roots accompanied by large seeds) may have always occurred within a specific divergence time, supporting effective mycorrhizal symbiosis and pathogen resistance.

We found that the positive relationship between root diameter and seed mass is stronger in non-woody plants than in woody plants (Extended Data Fig. 5), especially in temperate regions where most non-woody plants in the literature have been studied (Extended Data Fig. 9a). Non-woody plants typically exhibit lower mycorrhizal colonization rates than woody plants with the same absorptive root diameter[49], based on GRooT and literature data (Extended Data Fig. 9b,c). As a result, non-woody plants require larger-diameter absorptive roots than woody plants to achieve similar levels of mycorrhizal colonization, which would facilitate both mycorrhizal P uptake and defence against soil fungal pathogens. While previous studies have reported differences in absorptive roots between non-woody and woody plants[40], our study specifically explains the differences

https://doi.org/10.1038/s41477-025-02089-4

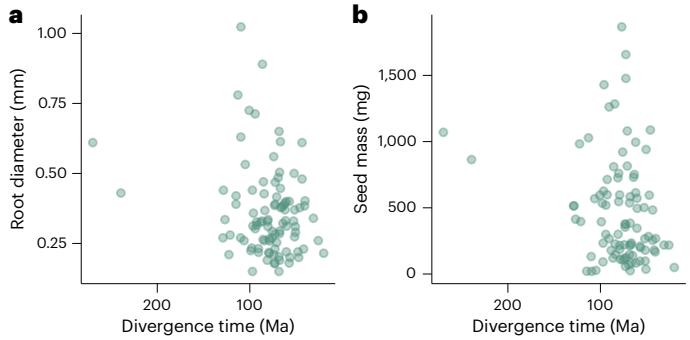

Fig. 6 | Evolutionary trends of absorptive root diameter and seed mass. Spearman correlations were conducted using our field-measured data. **a**,**b**, Absorptive root diameter (**a**) and seed mass (**b**) are both not significantly correlated with family divergence time (Ma, million years ago). For **a**, $r = 0.1$, $P = 0.319$, $n = 97$; for **b**, $r = 0.19$, $P = 0.066$, $n = 93$. Significance was tested using a two-sided *t*-test.

between non-woody and woody plants in terms of the root diameter–seed mass relationship, both of which traits could be driven by mycorrhizal associations.

Conclusions

In summary, by analysing the largest dataset on root traits and seed mass so far, we offer new insights into the connection between plant resource acquisition, reproduction by seeds and pathogen protection in seedlings. Specifically, we found that large seeds are associated with thick absorptive fine roots. This link does not result from enhanced resource transport by larger vessel areas. Instead, it arises from a larger cortical area, supporting mycorrhizal symbionts which, in turn, help mycorrhizal P uptake and/or defence against soil pathogens, ultimately improving seedling survival and influencing plant–soil feedbacks by affecting root morphology[49]. Furthermore, this potential duality of function raises questions about the multifunctionality hypothesis in ref. 50, which posits a trade-off between nutrient acquisition and pathogen defence, highlighting the need for more empirical studies to test this hypothesis. Our findings suggest practical applications in agriculture and forestry, such as selecting or cultivating AM plants with large seeds and hence thick absorptive roots to reduce negative plant–soil feedback through strong mycorrhizal association against soil pathogens. Importantly, this co-variation is strongly influenced by mycorrhizal type: it is present in AM plants but absent in ECM plants, probably due to an inherent difference in pathogen resistance between the two mycorrhizal types. The dual function of AM fungi in P uptake and pathogen defence offers a fresh perspective on how above- and belowground plant organs coordinate to shape whole-plant life-history strategies and their adaptation to heterogeneous environments. Understanding this coordination helps predict how plant species will perform and distribute themselves in environments that differ in P availability and pathogen load, particularly under global change. Finally, critical experiments are needed in the future to dissect the dual role of AM association as well as their relative contributions to the global coordination between root and seed traits.

Methods

Study sites

This study was conducted in 11 representative forest ecosystems across tropical (1 site), subtropical (5 sites) and temperate (5 sites) regions in China. The tropical forest we sampled here is the typical forest and the hotspot of plant diversity in China. To enable generalization of the results in the tropical forest, we collected the largest number of plant species in this forest across all the 11 sampling sites. Detailed information on the sampling sites and the number of species sampled can be found in Extended Data Table 1. We collected mature fruits and seeds of common woody plant species (trees and shrubs) from each site.

Sampling approach and trait measurements

We first measured the height of each sampled individual. Following the methods of ref. 51, we collected fruits and seeds[51]. For each plant species, more than three mature individuals were selected, and more than 50 mature fruits or seeds were collected from each individual plant, the number depending on how many fruits or seeds matured in the individual plant. For small-sized seeds, more than 100 seeds per plant species were collected. For species with limited or unavailable seed sources for collection, seeds were obtained from the Germplasm Bank of Wild Species in Southwest China. The fruit pulp or associated structures (for example, wind-dispersed appendages) were removed from each species, and seed size and dry weight were measured[52]. The dry mass of 30–50 seeds per species was measured (70 °C, >72 h); for small seeds, 100 seeds were measured, and for extremely small seeds, the weight per thousand seeds was used to calculate individual seed dry weight[51–54]. For each species, we also collected at least 30 intact and undamaged leaves from the upper canopy to measure leaf morphological and chemical traits[4]. Leaf area (LA, cm^2) was measured using a Li-3000C portable leaf area metre (Li-COR). Leaves were scanned, dried (60 °C for 48 h) and weighed to calculate specific leaf area (SLA, $cm^2\ g^{-1}$). Leaves were then ground and analysed for N concentration (LN%) using an elemental analyser (IR-MS, Thermo Fisher). Seed phosphorus concentration was measured for randomly selected 44 AM plant species and 28 ECM plant species following the Mo–Sb colorimetrical method after digestion of the seed samples with H_2SO_4–H_2O_2 (ref. 55).

Root samples were collected following established methods[24,31,41]. Lateral roots were traced from the main root of each tree, and branches containing at least five root orders were selected. Surface soil was carefully brushed off, and a portion of each root sample was washed with deionized water and placed in FAA solution (9 ml 70% ethanol, 9 ml deionized water, 1 ml formaldehyde and 1 ml acetic acid) for anatomical measurements. The remainder of the sample was stored on ice and transported to the laboratory for root morphological and chemical analyses[24,31,41,56].

In the laboratory, roots were cleaned with deionized water to isolate absorptive roots, specifically the 2–3 most distal root orders composed primarily of primary structures[24,31,41,56]. Some absorptive roots were scanned using a root scanner (Epson Perfection V700 Photo scanner, Epson), and root length, volume and diameter (RD, mm) were calculated using WinRHIZO software (WinRhizo Pro 2007d software, Regent). The roots were then dried (60 °C for several days) and weighed to calculate specific root length (SRL, $m\ g^{-1}$) and tissue density (RTD, $g\ cm^{-3}$). Another portion of the root sample was dried, ground and analysed for N concentration (Root N, %) using an elemental analyser (IR-MS, Thermo Fisher).

For each species, 15–20 first-order roots were selected from the FAA solution for anatomical analysis. The procedure involved dehydration with alcohol, clearing with xylene, embedding in paraffin, sectioning and staining. Sections were photographed under a microscope (Olympus BX-63), and cortical thickness (CT, μm), vessel diameter (VD, μm) and vessel density (VDen, n μm^{-2}) were measured using ImageJ software (NIH)[31,56,57].

We collected soil samples from Xishuangbanna Tropical Rainforest Nature Reserve, Dinghushan National Nature Reserve, Shennongjia National Nature Reserve, Jigongshan National Nature Reserve, Changbaishan National Nature Reserve, and Huzhong National Nature Reserve in the field according to the method described in ref. 46. We obtained data on soil fungal pathogens through sequencing. Fungal functional guilds for fungal operational taxonomic units (OTUs) were also assigned using FUNGuild according to refs. 45,46.

The global dataset collection

We obtained global data on fine root traits (including AM fungi colonization rates) from the GRooT database[41]. We obtained seed mass data from the TRY database[58] and from ref. 2. We also collected root and seed data not included in these databases from other published studies[2,26–28,59,60].

Mycorrhizal types of plant in both measured and collected datasets were determined on the basis of published studies and mycorrhizal classification databases[61–66]. For species whose mycorrhizal type was not confirmed in our databases and literature, we determined mycorrhizal type through field observations during sampling and anatomical analysis of root paraffin sections. For a few plant species with uncertain mycorrhizal type (15 species), we inferred the mycorrhizal type, as always done in previous studies, on the basis of the predominant mycorrhizal type within the genus[61,67]. Woody plants were classified into AM (757 species), ECM (140 species), ericoid mycorrhizal (ERM; 4 species), NM (10 species) or unknown (46 species). AM + ECM plant species were assigned to the ECM category on the basis of their ability to diverge from the ancestral stage of AM[66]. Non-woody plants were classified into AM (266 species), ECM (2 species) or unknown (29 species); AM + NM plant species were treated as AM because AM is favoured by natural selection in dual mycorrhizal associations[63]. Plant species with undetermined mycorrhizal status were not included in the analyses of the impacts of mycorrhizal types (AM versus ECM) on plant trait relationships.

Data analysis

We conducted type II linear regressions using standardized major axis (SMA) to explore the bivariate plant trait relationships. The trait data were $\log_{10}$ transformed before the SMA analysis to achieve normality. We used the 'sma' function in the 'smart' package to test differences in the SMA slopes between plant functional groups.

We first corrected species names and family information using The Plant List (http://www.theplantlist.org). Then, a phylogenetic tree was constructed using the 'U.PhyloMaker' package[68], following the APG IV phylogenetic system[69] for all analyses. On the basis of this phylogenetic tree, we calculated Blomberg's *K* using the 'Picante' package[70] to evaluate the phylogenetic influence on each trait; generally, a higher Blomberg's *K* indicates a greater phylogenetic influence[70]. Next, we performed trait correlation analysis excluding phylogenetic effects using the 'pgls' function in the 'caper' package[71] (Extended Data Fig. 6).

We conducted PCA using the 'factoextra' and 'funspace' packages to determine the major dimensions of trait variation among organs. Plant trait data were $\log_{10}$ transformed and standardized before the PCA to meet the requirement of normal distribution and variance homogeneity, respectively. To visualize the probability of a given trait appearing in PCA space, we constructed 2D kernel density plots with contours using the 'funspace' package[72] and added contour lines. The colour gradient and contours correspond to the 0.25, 0.5 and 0.99 quantiles of the trait space, highlighting areas with the corresponding probability of trait occurrence. We also assessed the evolutionary pattern of absorptive root diameter and seed mass using our field-measured data. Family-level values of root diameter and seed mass were assessed using the 'phytools' package and 'anc.ML' function. All statistical analyses and data visualizations were performed using R (v.4.3.2, R Core Team 2023)[73].

Reporting summary

Further information on research design is available in the Nature Portfolio Reporting Summary linked to this article.

Data availability

The raw data in this study are available in figshare (https://doi.org/10.6084/m9.figshare.28300658)[74]. Literature data were extracted from the Global Root Trait database (https://groot-database.github.io/GRooT/)[40].

Code availability

The code utilized for this study is publicly available and is hosted in figshare (https://doi.org/10.6084/m9.figshare.28300658)[74].

References

1. Díaz, S. et al. The global spectrum of plant form and function. *Nature* **529**, 167–171 (2016).
2. Carmona, C. P. et al. Fine-root traits in the global spectrum of plant form and function. *Nature* **597**, 683–687 (2021).
3. Wright, I. J. et al. The worldwide leaf economics spectrum. *Nature* **428**, 821–827 (2004).
4. Li, L. et al. Leaf economics and hydraulic traits are decoupled in five species-rich tropical-subtropical forests. *Ecol. Lett.* **18**, 899–906 (2015).
5. Zhang, Y. et al. The origin of bi-dimensionality in plant root traits. *Trends Ecol. Evol.* **39**, 78–88 (2024).
6. Bergmann, J. et al. The fungal collaboration gradient dominates the root economics space in plants. *Sci. Adv.* **6**, eaba3756 (2020).
7. Corner, E. J. H. The Durian theory or the origin of the modern tree. *Ann. Bot.* **13**, 367–414 (1949).
8. Reich, P. B. The world-wide 'fast–slow' plant economics spectrum: a traits manifesto. *J. Ecol.* **102**, 275–301 (2014).
9. Leishman, M., Wright, I., Moles, A. & Westoby, M. in *Seeds: The Ecology of Regeneration in Plant Communities* (ed. Fenner, M.) 31–57 (CABI, 2000).
10. Ma, Z. et al. The determination of leaf size on the basis of developmental traits. *New Phytol.* **246**, 461–480 (2025).
11. Weigelt, A. et al. The importance of trait selection in ecology. *Nature* **618**, E29–E30 (2023).
12. Weigelt, A. et al. An integrated framework of plant form and function: the belowground perspective. *New Phytol.* **232**, 42–59 (2021).
13. Zhang, P. P. et al. Contrasting coordination of non-structural carbohydrates with leaf and root economic strategies of alpine coniferous forests. *New Phytol.* **243**, 580–590 (2024).
14. Joswig, J. S. et al. Climatic and soil factors explain the two-dimensional spectrum of global plant trait variation. *Nat. Ecol. Evol.* **6**, 36–50 (2022).
15. Moles, A. T. et al. Global patterns in seed size. *Glob. Ecol. Biogeogr.* **16**, 109–116 (2007).
16. Zheng, J., Guo, Z. & Wang, X. Seed mass of angiosperm woody plants better explained by life history traits than climate across China. *Sci. Rep.* **7**, 2741 (2017).
17. Fricke, E. C., Ordonez, A., Rogers, H. S. & Svenning, J.-C. The effects of defaunation on plants' capacity to track climate change. *Science* **375**, 210–214 (2022).
18. Leslie, A. B., Beaulieu, J. M. & Mathews, S. Variation in seed size is structured by dispersal syndrome and cone morphology in conifers and other nonflowering seed plants. *New Phytol.* **216**, 429–437 (2017).
19. Marchand, P. et al. Seed-to-seedling transitions exhibit distance-dependent mortality but no strong spacing effects in a Neotropical forest. *Ecology* **101**, e02926 (2020).
20. Bergmann, J., Ryo, M., Prati, D., Hempel, S. & Rillig, M. C. Root traits are more than analogues of leaf traits: the case for diaspore mass. *New Phytol.* **216**, 1130–1139 (2017).
21. Copeland, L. O. & McDonald, M. B. in *Principles of Seed Science and Technology* (eds Copeland, L. O. & McDonald, M. B.) 58–71 (Springer, 2001).
22. Van Der Heijden, M. G. A. in *Mycorrhizal Ecology* (eds van der Heijden, M. G. A. & Sanders, I. R.) 243–265 (Springer, 2003).
23. Nallathambi, P. et al. in *Seed-borne Diseases of Agricultural Crops: Detection, Diagnosis and Management* (eds Kumar, R. & Gupta, A.) 749–791 (Springer, 2020).

24. Kong, D. et al. Leading dimensions in absorptive root trait variation across 96 subtropical forest species. *New Phytol.* **203**, 863–872 (2014).
25. Liang, M. et al. Arbuscular mycorrhizal fungi counteract the Janzen-Connell effect of soil pathogens. *Ecology* **96**, 562–574 (2015).
26. Zangaro, W., Nishidate, F. R., Camargo, F. R. S., Romagnoli, G. G. & Vandressen, J. Relationships among arbuscular mycorrhizas, root morphology and seedling growth of tropical native woody species in southern Brazil. *J. Trop. Ecol.* **21**, 529–540 (2005).
27. Laughlin, D. C., Leppert, J. J., Moore, M. M. & Sieg, C. H. A multi-trait test of the leaf-height-seed plant strategy scheme with 133 species from a pine forest flora. *Funct. Ecol.* **24**, 493–501 (2010).
28. Siqueira, J. O. & Saggin-Júnior, O. J. Dependency on arbuscular mycorrhizal fungi and responsiveness of some Brazilian native woody species. *Mycorrhiza* **11**, 245–255 (2001).
29. West, G. B., Brown, J. H. & Enquist, B. J. A general model for the structure and allometry of plant vascular systems. *Nature* **400**, 664–667 (1999).
30. Brown, J. H., Gillooly, J. F., Allen, A. P., Savage, V. M. & West, G. B. Toward a metabolic theory of ecology. *Ecology* **85**, 1771–1789 (2004).
31. Kong, D. et al. Nonlinearity of root trait relationships and the root economics spectrum. *Nat. Commun.* **10**, 2203 (2019).
32. Swamy, V. et al. Are all seeds equal? Spatially explicit comparisons of seed fall and sapling recruitment in a tropical forest. *Ecol. Lett.* **14**, 195–201 (2011).
33. Puerta-Piñero, C., Muller-Landau, H. C., Calderón, O. & Wright, S. J. Seed arrival in tropical forest tree fall gaps. *Ecology* **94**, 1552–1562 (2013).
34. Im, C., Chung, J., Kim, H. S., Chung, S. & Yoon, T. K. Are seed dispersal and seedling establishment distance- and/or density-dependent in naturally regenerating larch patches? A within-patch scale analysis using an eigenvector spatial filtering approach. *For. Ecol. Manage.* **531**, 120763 (2023).
35. Connell, J. H. in *Dynamics of Numbers in Populations* (eds den Boer, P. J & Gradwell, G. R.) 298–312 (Centre for Agricultural Publishing and Documentation, 1971).
36. Hülsmann, L. et al. Latitudinal patterns in stabilizing density dependence of forest communities. *Nature* **627**, 564–571 (2024).
37. Hou, S. et al. A microbiota-root-shoot circuit favours *Arabidopsis* growth over defence under suboptimal light. *Nat. Plants* **7**, 1078–1092 (2021).
38. Marx, D. H. Ectomycorrhizae as biological deterrents to pathogenic root infections. *Annu. Rev. Phytopathol.* **10**, 429–454 (1972).
39. Brundrett, M., Murase, G. & Kendrick, B. Comparative anatomy of roots and mycorrhizae of common Ontario trees. *Botany* **68**, 551–578 (1990).
40. Guerrero-Ramírez, N. R. et al. Global root traits (GRooT) database. *Glob. Ecol. Biogeogr.* **30**, 25–37 (2021).
41. Ma, Z. et al. Evolutionary history resolves global organization of root functional traits. *Nature* **555**, 94–97 (2018).
42. Janos, D. P. Vesicular-arbuscular mycorrhizae affect lowland tropical rain forest plant growth. *Ecology* **61**, 151–162 (1980).
43. Peat, H. J. & Fitter, A. H. The distribution of arbuscular mycorrhizas in the British flora. *New Phytol.* **125**, 845–854 (1993).
44. Hennecke, J. et al. Responses of rhizosphere fungi to the root economics space in grassland monocultures of different age. *New Phytol.* **240**, 2035–2048 (2023).
45. Tedersoo, L. et al. Global diversity and geography of soil fungi. *Science* **346**, 1256688 (2014).
46. Hu, Y. et al. Contrasting latitudinal diversity and co-occurrence patterns of soil fungi and plants in forest ecosystems. *Soil Biol. Biochem.* **131**, 100–110 (2019).
47. Reich, P. B. & Oleksyn, J. Global patterns of plant leaf N and P in relation to temperature and latitude. *Proc. Natl Acad. Sci. USA* **101**, 11001–11006 (2004).
48. Wang, M. et al. Molecular-level carbon traits underlie the multidimensional fine root economics space. *Nat. Plants* **10**, 901–909 (2024).
49. Misra, V. & Mall, A. K. in *Plant Endophytes and Secondary Metabolites* (eds Egamberdieva, D. et al.) 81–94 (Academic Press, 2024).
50. Newsham, K. K., Fitter, A. H. & Watkinson, A. R. Multi-functionality and biodiversity in arbuscular mycorrhizas. *Trends Ecol. Evol.* **10**, 407–411 (1995).
51. Schneider, G. F., Salazar, D., Hildreth, S. B., Helm, R. F. & Whitehead, S. R. Comparative metabolomics of fruits and leaves in a hyperdiverse lineage suggests fruits are a key incubator of phytochemical diversification. *Front. Plant Sci.* **12**, 693739 (2021).
52. Wang, B., Phillips, J. S. & Tomlinson, K. W. Tradeoff between physical and chemical defense in plant seeds is mediated by seed mass. *Oikos* **127**, 440–447 (2018).
53. Li, Y.-L. et al. Seed traits of reintroduced invasive populations of *Triadica sebifera* show few differences in comparison with those of native populations. *Plant Ecol.* **224**, 697–703 (2023).
54. Cheng, J. et al. Seed traits and burial state affect plant seed secondary dispersal mediated by rodents. *Heliyon* **10**, e32612 (2024).
55. Kong, D. et al. Plant functional group removal alters root biomass and nutrient cycling in a typical steppe in Inner Mongolia, China. *Plant Soil* **316**, 133–144 (2011).
56. Long, Y., Kong, D., Chen, Z. & Zeng, H. Variation of the linkage of root function with root branch order. *PLoS ONE* **8**, e57153 (2013).
57. Guo, D. et al. Anatomical traits associated with absorption and mycorrhizal colonization are linked to root branch order in twenty-three Chinese temperate tree species. *New Phytol.* **180**, 673–683 (2008).
58. Kattge, J. et al. TRY plant trait database – enhanced coverage and open access. *Glob. Change Biol.* **26**, 119–188 (2020).
59. Wright, I. J. & Westoby, M. Differences in seedling growth behaviour among species: trait correlations across species, and trait shifts along nutrient compared to rainfall gradients. *J. Ecol.* **87**, 85–97 (1999).
60. Mueller, K. E., Kray, J. A. & Blumenthal, D. M. Coordination of leaf, root, and seed traits shows the importance of whole plant economics in two semiarid grasslands. *New Phytol.* **241**, 2410–2422 (2024).
61. Wang, B. & Qiu, Y. L. Phylogenetic distribution and evolution of mycorrhizas in land plants. *Mycorrhiza* **16**, 299–363 (2006).
62. Akhmetzhanova, A. A. et al. A rediscovered treasure: mycorrhizal intensity database for 3000 vascular plant species across the former Soviet Union. *Ecology* **93**, 689–690 (2012).
63. Maherali, H., Oberle, B., Stevens, P. F., Cornwell, W. K. & McGlinn, D. J. Mutualism persistence and abandonment during the evolution of the mycorrhizal symbiosis. *Am. Nat.* **188**, E113–E125 (2016).
64. Brundrett, M. & Tedersoo, L. Misdiagnosis of mycorrhizas and inappropriate recycling of data can lead to false conclusions. *New Phytol.* **221**, 18–24 (2019).
65. Soudzilovskaia, N. A. et al. FungalRoot: global online database of plant mycorrhizal associations. *New Phytol.* **227**, 955–966 (2020).
66. Valverde-Barrantes, O. J., Freschet, G. T., Roumet, C. & Blackwood, C. B. A worldview of root traits: the influence of ancestry, growth form, climate and mycorrhizal association on the functional trait variation of fine-root tissues in seed plants. *New Phytol.* **215**, 1562–1573 (2017).
67. Sun, T., Zhang, H. & Wang, Z. Reply to Tedersoo et al.: Plant species within the same family or genus can have different mycorrhizal types? *Proc. Natl Acad. Sci. USA* **116**, 12141–12142 (2019).

68. Jin, Y. & Qian, H. U. PhyloMaker: an R package that can generate large phylogenetic trees for plants and animals. *Plant Divers.* **45**, 347–352 (2023).
69. The Angiosperm Phylogeny Group et al. An update of the Angiosperm Phylogeny Group classification for the orders and families of flowering plants: APG IV. *Bot. J. Linn. Soc.* **181**, 1–20 (2016).
70. Blomberg, S. P. & Garland Jr, T. Tempo and mode in evolution: phylogenetic inertia, adaptation and comparative methods. *J. Evol. Biol.* **15**, 899–910 (2002).
71. Orme, D. et al. CAPER: comparative analyses of phylogenetics and evolution in R. R package version 0.5.2 https://github.com/davidorme/caper (2012).
72. Carmona, C. P., Pavanetto, N. & Puglielli, G. funspace: an R package to build, analyse and plot functional trait spaces. *Divers. Distrib.* **30**, e13820 (2024).
73. R Core Team. *R: A Language and Environment for Statistical Computing* (R Foundation for Statistical Computing, 2013); http://www.R-project.org/
74. Yang, Q. et al. Arbuscular mycorrhizal association regulates global root-seed coordination. *figshare* https://doi.org/10.6084/m9.figshare.28300658 (2025).

Acknowledgements

We thank S. Chen for comments on an early draft of the manuscript; J. Bergmann for discussion of the idea regarding hypothesis 2 in the early draft; J. Chen, J. Cao, M. Han, H. Wang, Y. Hou, Y. Tian, Y. Dong, M. Liu, D. Mo, C. Xiang, Y. Jiang, Y. Liang, S. Dong, Z. Meng, L. Zhao and C. Hu for assistance in field sampling. We also thank the following field research stations and government agencies for their kind support: Xishuangbanna Station for Tropical Forest Studies of Xishuangbanna Tropical Botanical Garden; Dinghushan Station for Subtropical Forest Studies of South China Botany Garden; Gutianshan Biodiversity Science Research Station; Shennongjia National Park Administration; Forest Ecosystem Research Station, Institute of Botany, Chinese Academy of Sciences; Beijing Forest Ecosystem Research Station, Chinese Academy of Sciences; Liangshui Experimental Forest Farm, Northeast Forestry University; Changbai Mountain Forest Ecosystem Positioning Station, Chinese Academy of Sciences. This study was supported by the National Natural Science Foundation of China (32471824, 32171746 and 31870522) to D.K., the leading talents of basic research in Henan Province (24XM0375) to D.K., Excellent Youth Creative Research Group Project in Henan Province (252300421002) to D.K., Foreign Scientists Studio in Henan Province (GZS2025011) to D.K., the Scientific Research Foundation of Henan Agricultural University (30500854) to D.K., the National Natural Science Foundation of China (42122054 and 42477227) to J.W., the Guangdong Provincial Key Laboratory of Soil and Groundwater Pollution Control (2023B1212060002) to J.W., the High-level University Special Fund (G030290001) to J.W., the National Natural Science Foundation of China (42077450) to Y. Z. and the Estonian Research Council (PRG2142) to C.P.C.

Author contributions

Q.Y. and D.K. conceived of the idea. Q.Y. and B.G. completed the creation of figures. Q.Y., D.K., M.L. and P.B.R. conducted the statistical analyses. Q.Y., D.K., J.W., G.L., H.W. and Y.L. discussed and contributed to the final framework of this study. Q.Y and D.K. wrote the first draft of the paper with significant help from P.K., R.D.B., J.H.C.C., S.D., I.J.W. and J.A.H. Q.Y., B.G., M.L., Y.L., P.K., P.B.R., R.D.B., J.H.C.C., N.J.B.K., S.D., I.J.W., N.H., J.A.H., Y.P., Q.H., Z.L., Z.W., W.Y., J.D., Z.Y., H.W., C.P.C., O.J.V.-B., D.L., J.C., H.Z., Y. Zhang, W.R., Y. Zhao, X.Y., G.F., J.W., G.L. and D.K. contributed to the completion and revision of the paper.

Competing interests

The authors declare no competing interests.

Additional information

Extended data is available for this paper at https://doi.org/10.1038/s41477-025-02089-4.

Supplementary information The online version contains supplementary material available at https://doi.org/10.1038/s41477-025-02089-4.

Correspondence and requests for materials should be addressed to Junjian Wang, Guoyong Li or Deliang Kong.

Peer review information *Nature Plants* thanks Wenming Bai, Christina Birnbaum and Thomas Kuyper for their contribution to the peer review of this work.

[1]College of Forestry, Henan Agricultural University, Zhengzhou, China. [2]Department of Environmental Studies, New York University, New York, NY, USA. [3]Key Laboratory of Wetland Ecology and Environment, Northeast Institute of Geography and Agroecology, Chinese Academy of Sciences, Changchun, China. [4]Department of Forest Mycology and Plant Pathology, Swedish University of Agricultural Sciences, Uppsala, Sweden. [5]Department of Forest Ecology and Management, Swedish University of Agricultural Sciences, Umeå, Sweden. [6]Department of Forest Resources, University of Minnesota St Paul, Minneapolis, MN, USA. [7]Institute for Global Change Biology and School for Environment and Sustainability, University of Michigan, Ann Arbor, MI, USA. [8]Hawkesbury Institute for the Environment, Western Sydney University, Penrith, New South Wales, Australia. [9]Lancaster Environment Centre, Lancaster University, Lancaster, UK. [10]Systems Ecology, A-LIFE, Vrije Universiteit, Amsterdam, the Netherlands. [11]Department of Ecology and Evolutionary Biology, University of California, Los Angeles, Los Angeles, CA, USA. [12]Instituto Multidisciplinario de Biología Vegetal (IMBIV), CONICET, Córdoba, Argentina. [13]FCEFyN, Universidad Nacional de Córdoba, Córdoba, Argentina. [14]School of Natural Sciences, Macquarie University, Sydney, New South Wales, Australia. [15]Key Laboratory of Sustainable Forest Ecosystem Management - Ministry of Education, Northeast Forest University, Harbin, China. [16]Department of Ecology and Conservation Biology, Texas A&M University, College Station, TX, USA. [17]College of Landscape Architecture and Art, Henan Agricultural University, Zhengzhou, China. [18]School of Life Sciences, Taizhou University, Taizhou, China. [19]College of Ecology and Environment, Zhengzhou University, Zhengzhou, China. [20]School of Life Sciences, Henan University, Kaifeng, China. [21]Institute of Ecology and Earth Sciences, University of Tartu, Tartu, Estonia. [22]International Center of Tropical Botany, Institute of Environment, Department of Biology, Florida International University, Miami, FL, USA. [23]Center for Interdisciplinary Biodiversity Research and College of Forestry, Shandong Agricultural University, Tai'an, China.

[24]Germplasm Bank of Wild Species and Yunnan Key Laboratory of Crop Wild Relatives Omics, Kunming Institute of Botany, Chinese Academy of Sciences, Kunming, China. [25]College of Urban and Environmental Sciences, Peking University, Beijing, China. [26]State Key Laboratory of Soil Pollution Control and Safety, Southern University of Science and Technology, Shenzhen, China. [27]Guangdong Provincial Key Laboratory of Soil and Groundwater Pollution Control, School of Environmental Science and Engineering, Southern University of Science and Technology, Shenzhen, China.
✉e-mail: wangjj@sustech.edu.cn; ligy535@henu.edu.cn; deliangkong1999@126.com

https://doi.org/10.1038/s41477-025-02089-4

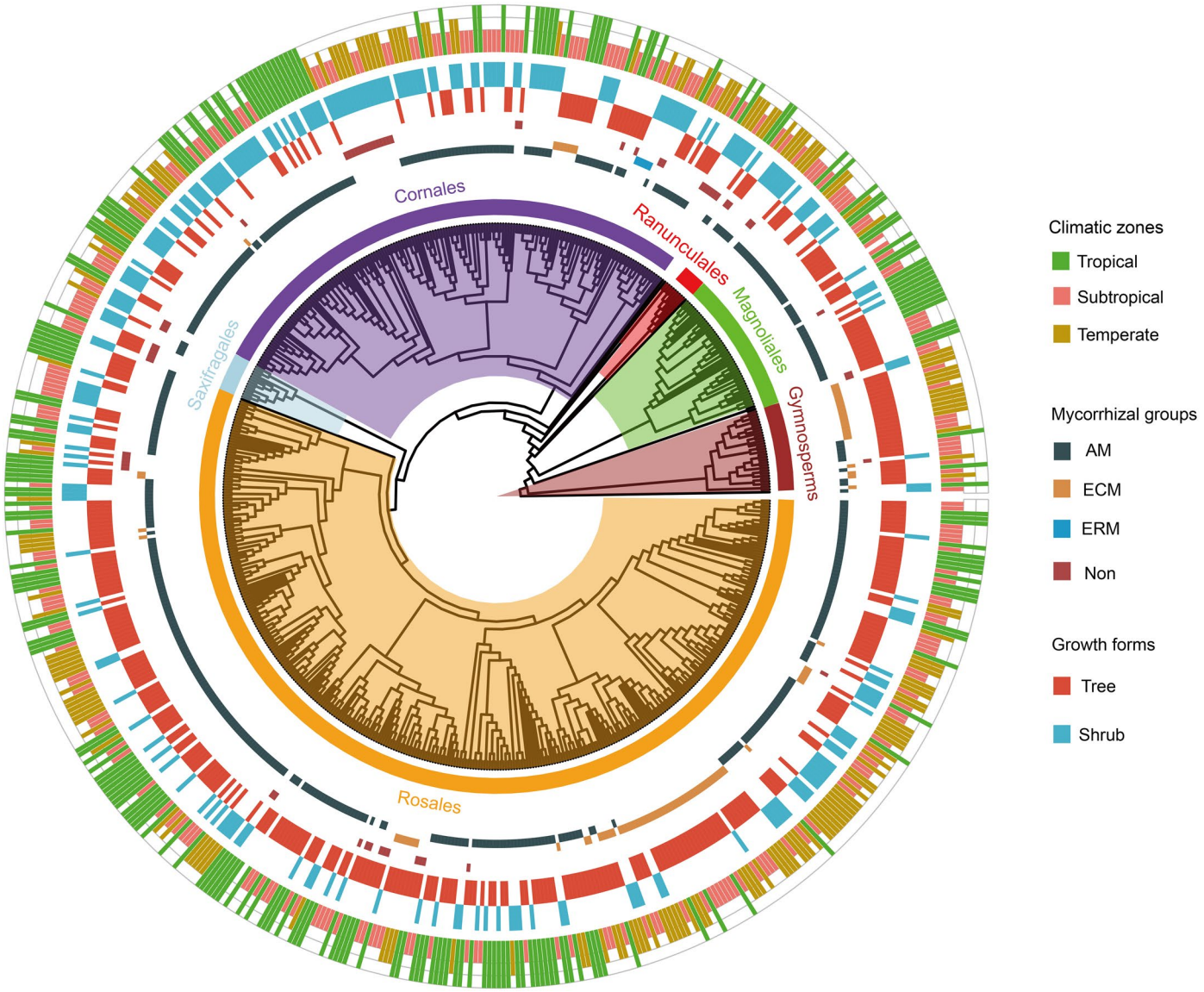

Extended Data Fig. 1 | Phylogenetic tree of 626 taxa in the study. The internal purple section of the phylogeny corresponds to the Cornales, the red section to the Ranunculales, the green section to the Magnoliales, the coffee-colored section to the Gymnosperms, the yellow section to the Rosales, and the blue section to the Saxifragales. The various color bars on the outside of the phylogeny's inner circle correspond to the mycorrhizal group, growth form, and climatic zone (in that order from inside to outside) of the respective plant species (the tips of the phylogeny). AM = arbuscular mycorrhizal; ECM = ectomycorrhizal; ERM = ericoid mycorrhizal; Non = unknown / non-mycorrhizal. Due to the limited number of ERM species, we only use AM and ECM species in our analysis.

https://doi.org/10.1038/s41477-025-02089-4

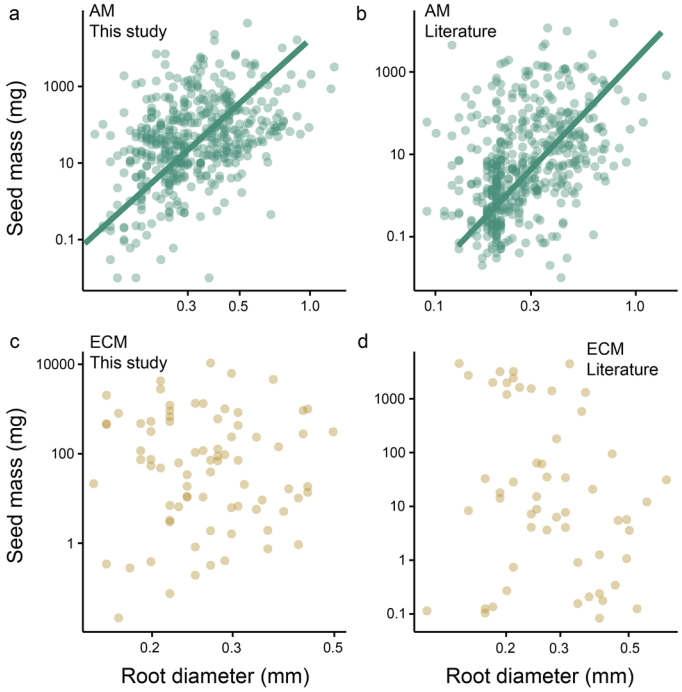

Extended Data Fig. 2 | Relationships between root diameter and seed mass. Analyses were performed using our field-measured trait data of this study (**a**, **c**) and existing data from the literature (**b**, **d**) using the standardized major axis (SMA) regression. For arbuscular mycorrhizal (AM) plant species, a significant positive correlation is shown: Field-measured data (**a**): Green filled circles; regression equation: $\log_{10}(y) = 5.80 \log_{10}(x) + 4.46$, $r = 0.43$, $P = 2.2 \times 10^{-16}$, $n = 489$. Literature data: (**b**): Tan filled circles; regression equation: $\log_{10}(y) = 6.10 \log_{10}(x) + 4.41$, $r = 0.43$, $P = 2.2 \times 10^{-16}$, $n = 506$. The scaling exponent for the field-measured data (**a**) is 5.80 (95% confidence interval (CI) = 5.35–6.28), equivalent to the exponent derived from the literature data (**b**) (6.10; 95% CI = 5.61–6.57) ($P = 2.22 \times 10^{-16}$; see the Method section). In contrast, no significant correlation was found for ectomycorrhizal (ECM) plant species: Field-measured data (**c**): Tan filled circles; $r = 0.01$, $P = 0.91$, $n = 78$. Literature data (**d**): Tan filled circles; $r = 0.24$, $P = 0.07$, $n = 55$. Significance was tested using a two-sided t-test. All data are plotted on logarithmic scales ($\log_{10}$) for both axes, with each point representing a single plant species.

https://doi.org/10.1038/s41477-025-02089-4

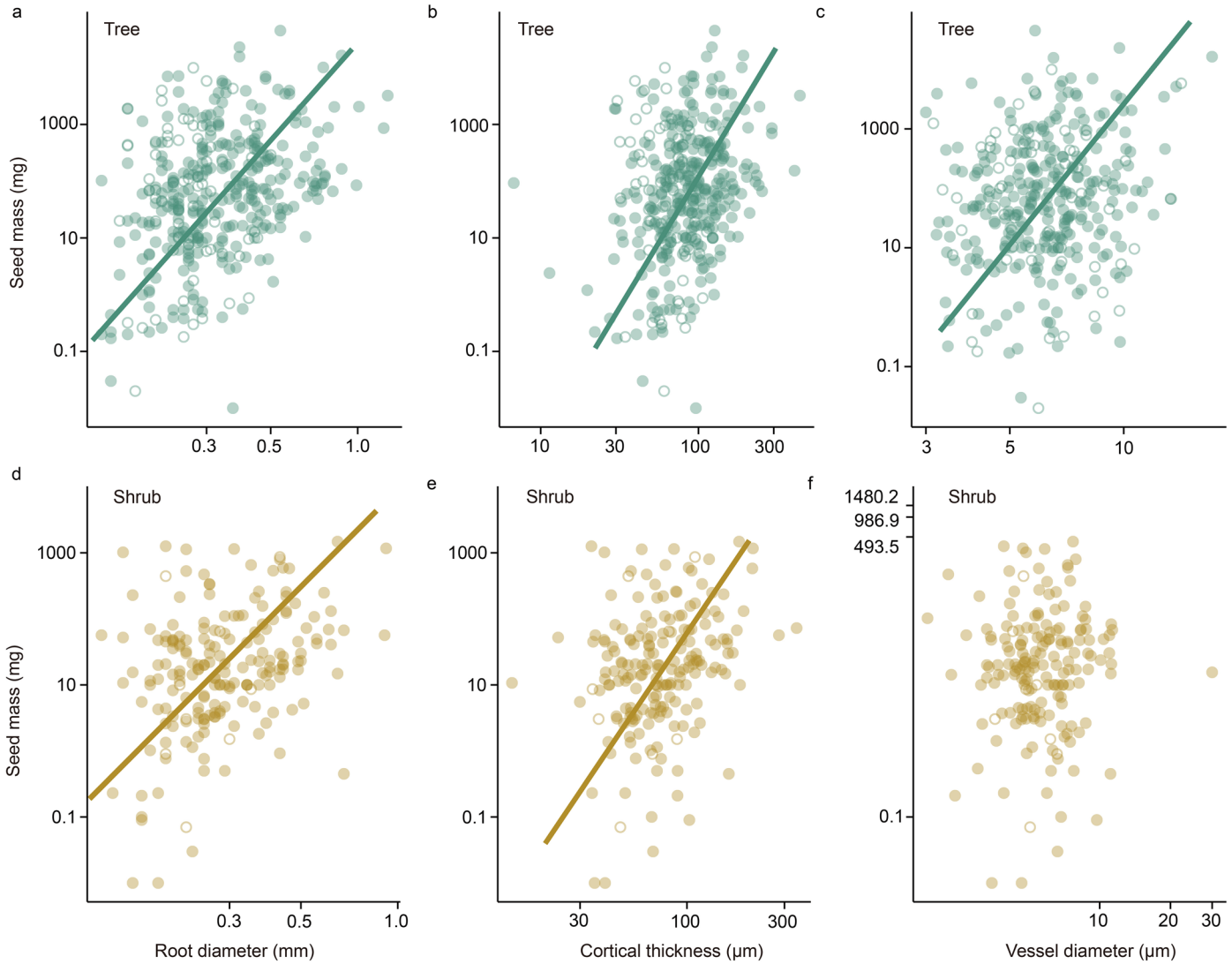

Extended Data Fig. 3 | Relationships between root anatomical traits and seed mass for different plant growth forms and mycorrhizal types. Analyses were performed using field-measured data using the standardized major axis (SMA) regression. There is a significant positive relationship between seed mass and root diameter in arbuscular mycorrhizal (AM) tree and shrub species (green filled circles; **a**, $\log_{10}(y) = 5.75 \log_{10}(x) + 4.51$, $r = 0.40$, $P = 2.24 \times 10^{-13}$, 95% CI = 5.19–6.38, $n = 303$; tan filled circles, **d**, $\log_{10}(y) = 5.55 \log_{10}(x) + 4.21$, $r = 0.38$, $P = 6.70 \times 10^{-6}$, 95% CI = 4.85–6.34, $n = 186$). The cortical thickness and seed mass of AM plant species show a positive relationship across two growth forms (green filled circles, **b**, $\log_{10}(y) = 4.73 \log_{10}(x) - 7.34$, $r = 0.33$, $P = 1.26 \times 10^{-9}$, 95% CI = 4.25–5.26, $n = 303$; tan filled circles; **e**, $\log_{10}(y) = 4.63 \log_{10}(x) - 7.40$, $r = 0.26$, $P = 0.0003$, 95% CI = 4.02–5.33, $n = 185$). The vessel diameter and seed mass is positively correlated only in tree species (green filled circles, **c**, $\log_{10}(y) = 7.82 \log_{10}(x) - 4.37$, $r = 0.20$, $P = 0.0006$, 95% CI = 6.98–8.78, $n = 283$), but not in shrub species (tan filled circles, **f**, $r = 0.05$, $P = 0.51$, $n = 175$). Conditional correlations by considering the significant relationship between cortical thickness and vessel diameter ($r = 0.52$, $P < 0.01$) shows no correlation between vessel diameter and seed mass ($r = 0.03$, $P = 0.49$) but a positive correlation between cortical thickness and seed mass ($r = 0.22$, $P < 0.01$). In contrast, no correlation is observed for ectomycorrhizal (ECM) species (green open circles, **a**, $r = 0.05$, $P = 0.73$, $n = 62$; **b**, $r = 0.18$, $P = 0.15$, $n = 62$; **c**, $r = 0.01$, $P = 0.92$, $n = 57$; tan open circles, **d**, $r = 0.09$, $P = 0.73$, $n = 16$; **e**, $r = 0.44$, $P = 0.09$, $n = 16$; **f**, $r = 0.13$, $P = 0.67$, $n = 14$). Significance was tested using a two-sided t-test. Data are plotted on a logarithmic scale ($\log_{10}$) for both axes, with each point representing one species.

https://doi.org/10.1038/s41477-025-02089-4

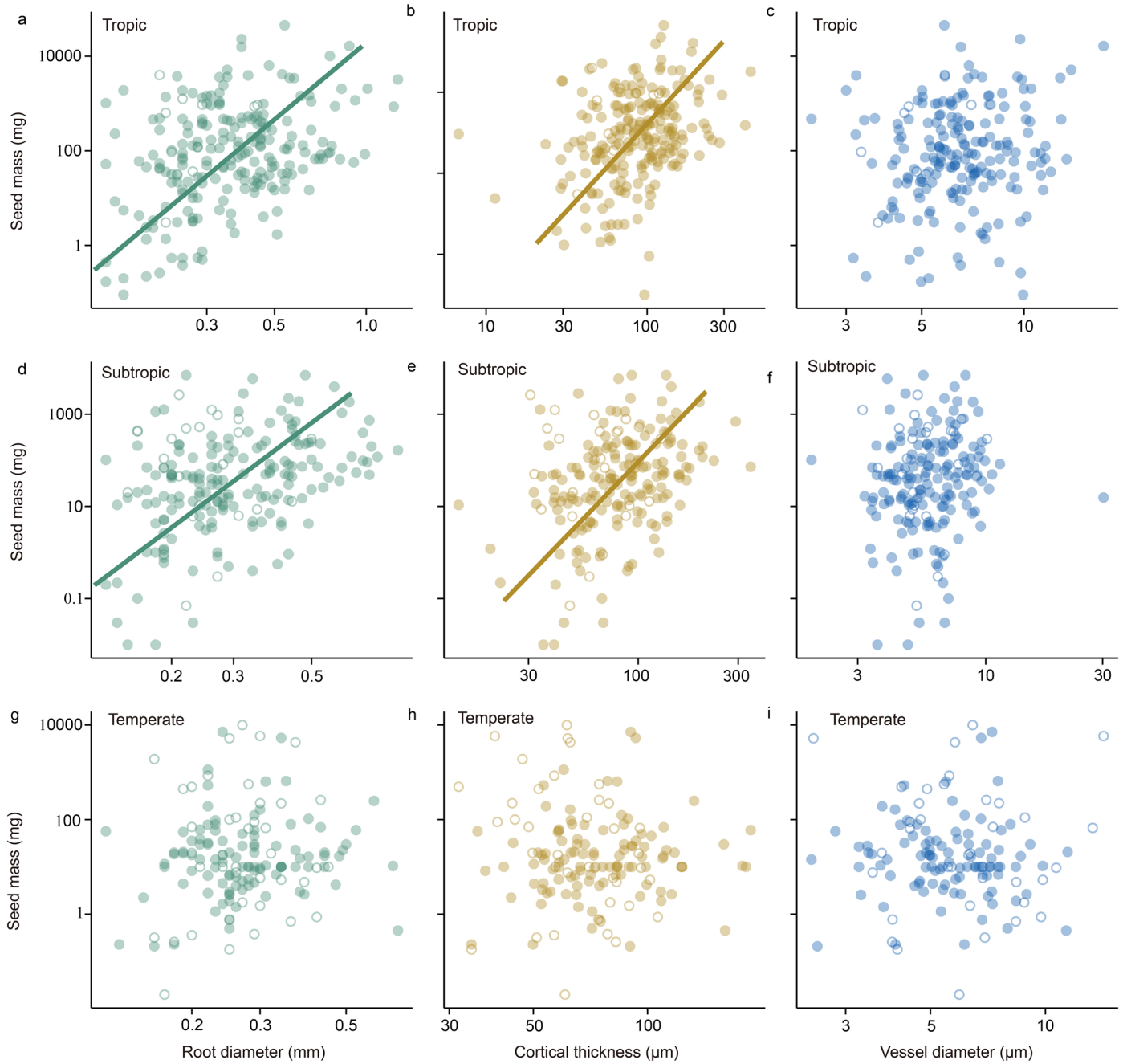

Extended Data Fig. 4 | Relationships between root traits and seed mass of different mycorrhizal types across different climatic zones. Analyses were performed using field-measured data using the standardized major axis (SMA) regression. Seed mass with both root diameter and cortical thickness of arbuscular mycorrhiza (AM) plant species are positively correlated in tropics and subtropics (green filled circles, **a**, $\log_{10}(y) = 5.72 \log_{10}(x) + 4.42$, $r = 0.38$, $P = 1.83 \times 10^{-8}$, 95% CI = 5.04–6.50, $n = 206$; **d**, $\log_{10}(y) = 5.80 \log_{10}(x) + 4.50$, $r = 0.44$, $P = 5.88 \times 10^{-10}$, 95% CI = 5.08–6.63, $n = 177$; tan filled circles, **b**, $\log_{10}(y) = 4.40 \log_{10}(x) - 6.61$, $r = 0.31$, $P = 4.58 \times 10^{-6}$, 95% CI = 3.86–5.01, $n = 206$; **e**, $\log_{10}(y) = 4.76 \log_{10}(x) - 7.56$, $r = 0.38$, $P = 1.92 \times 10^{-7}$, 95% CI = 4.15–5.46, $n = 177$), but not in temperate (green filled circles, **g**, $r = 0.17$, $P = 0.09$, $n = 106$. tan filled circles, **h**, $r = 0.1$, $P = 0.31$, $n = 105$). In contrast, no correlation is observed for ectomycorrhizal (ECM) plant species (green open circles, **a**, $R^2 = 0.27$, $P = 0.45$, $n = 10$; **d**, $r = 0.12$, $P = 0.57$, $n = 25$; **g**, $r = 0.07$, $P = 0.65$, $n = 43$; tan open circles, **b**, $r = 0.48$, $P = 0.16$, $n = 10$; **e**, $r = 0.08$, $P = 0.71$, $n = 25$; **h**, $r = 0.29$, $P = 0.06$, $n = 43$). The vessel diameter and seed mass of AM and ECM plant species show no correlation across three climatic zones (blue filled circles, **c**, $r = 0.13$, $P = 0.07$, $n = 192$; **f**, $r = 0.15$, $P = 0.052$, $n = 170$; **i**, $r = 0.002$, $P = 0.95$, $n = 96$; blue open circles, **c**, $r = 0.62$, $P = 0.10$, $n = 8$; **f**, $r = 0.06$, $P = 0.79$, $n = 24$; **i**, $r = 0.06$, $P = 0.68$, $n = 39$). Significance was tested using a two-sided t-test. Data are plotted on a logarithmic scale ($\log_{10}$) for both axes, with each point representing one species.

https://doi.org/10.1038/s41477-025-02089-4

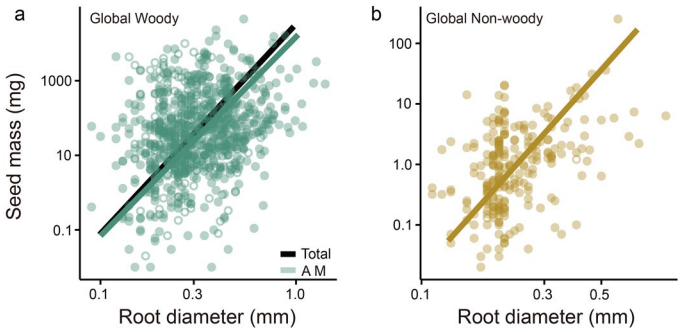

Extended Data Fig. 5 | Relationships between root diameter and seed mass for global woody and non-woody species. Analyses were performed using field-measured data of this study and literature data using the standardized major axis (SMA) regression. There is a positive correlation between root diameter and seed mass in global woody arbuscular mycorrhizal (AM) and ectomycorrhizal (ECM) plant species (AM + ECM) plant species (Total, **a**, $\log_{10}(y) = 5.93 \log_{10}(x) + 4.52$, $r = 0.26$, $P = 2.2 \times 10^{-16}$, CI = 5.56–6.33, $n = 854$). The positive correlation between root diameter and seed mass persists for both global woody and non-woody AM plant species (green filled circles, **a**, $\log_{10}(y) = 5.55 \log_{10}(x) + 4.27$, $r = 0.31$, $P = 2.2 \times 10^{-16}$, $n = 729$; tan filled circles, **b**, $\log_{10}(y) = 4.76 \log_{10}(x) + 4.26$, $r = 0.41$, $P = 2.79 \times 10^{-12}$, $n = 266$). For global woody AM plant species, the scaling exponent is 5.55 (95% (CI) = 5.18–5.95), which is significantly different from that of global non-woody AM plant species (exponent = 4.76, 95% CI = 4.26–5.31) ($P = 2.22 \times 10^{-16}$, see the Methods section). In contrast, no correlation is observed for ECM woody plant species (green open circles, **a**, $r = 0.14$, $P = 0.11$, $n = 137$). Non-woody ECM plant species are not analyzed due to the limited number of species. Significance was tested using a two-sided *t*-test. Data are presented on logarithmic scales ($\log_{10}$) for both axes, with each point representing one species.

https://doi.org/10.1038/s41477-025-02089-4

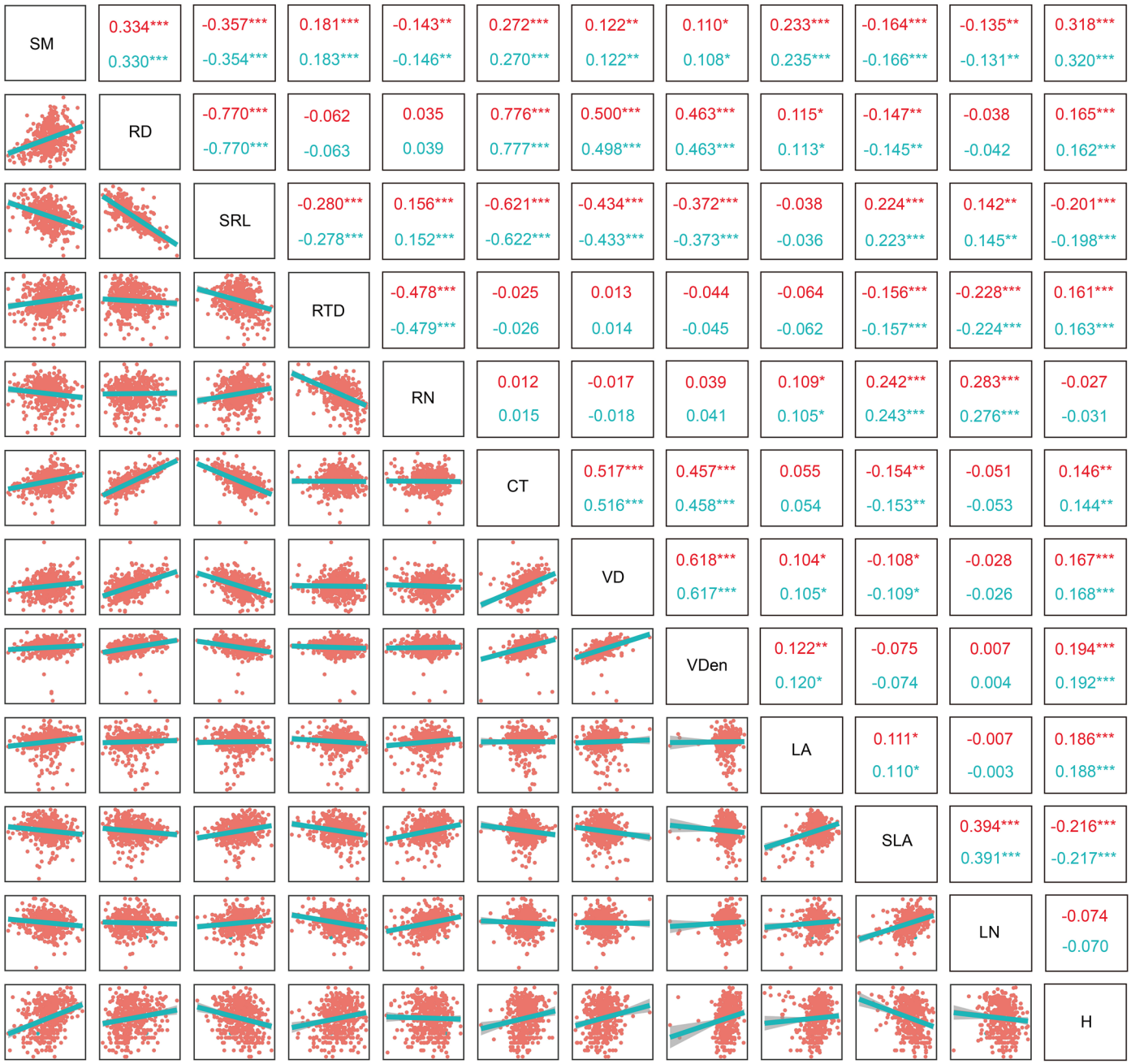

Extended Data Fig. 6 | Pairwise correlations for all plant traits used in this study. Analyses were performed using field-measured data of this study. In each scatter plot, the blue scatter is represented by the raw data, and the red scatter is represented by PGLS data (removal of the phylogenetic signal). SM - seed mass, RD - root diameter, SRL - specific root length, RTD - root tissue density, RN- root nitrogen concentration, CT - root cortical thickness, VD – root vessel diameter, VDen – root vessel density, LA - single leaf area, SLA – specific leaf area, LN - leaf nitrogen concentration, and H - height of mature plants. Regression lines represent raw data correlations (blue) and phylogenetically-corrected bivariate relationships calculated by fitting Phylogenetic Generalized Least Square models (red). Correlation coefficients are obtained using Pearson correlation, with the raw data shown in blue and the phylogenetic correction data in red (* $0.05 > P > 0.01$; ** $0.01 > P > 0.001$; *** $P < 0.001$) Note that the two regression lines and scatter points are too close to be distinguished by the naked eye.

https://doi.org/10.1038/s41477-025-02089-4

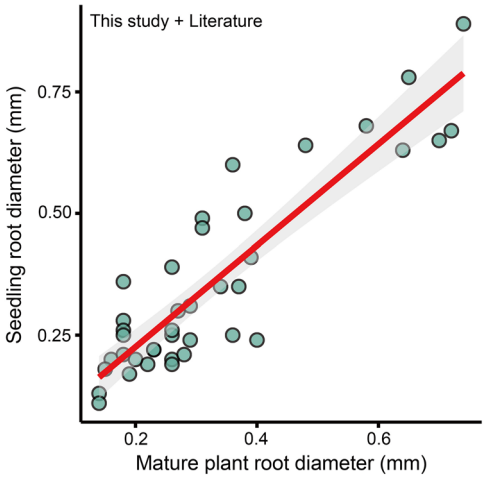

Extended Data Fig. 7 | Relationships between mature plant root diameter and seedling root diameter of a same plant species. Pearson correlation is conducted using our field-measured data and literature data (Siqueira and Saggin-Júnior[28]). There is a positive relationship between root diameter of mature plants and root diameter of seedlings ($y = 1.04x + 0.02$, $r = 0.89$, $P = 2.14 \times 10^{-12}$, $n = 39$). Shaded areas indicates 95% confidence intervals of the regression lines. Significance was tested using a two-sided t-test. Each point represents one species.

https://doi.org/10.1038/s41477-025-02089-4

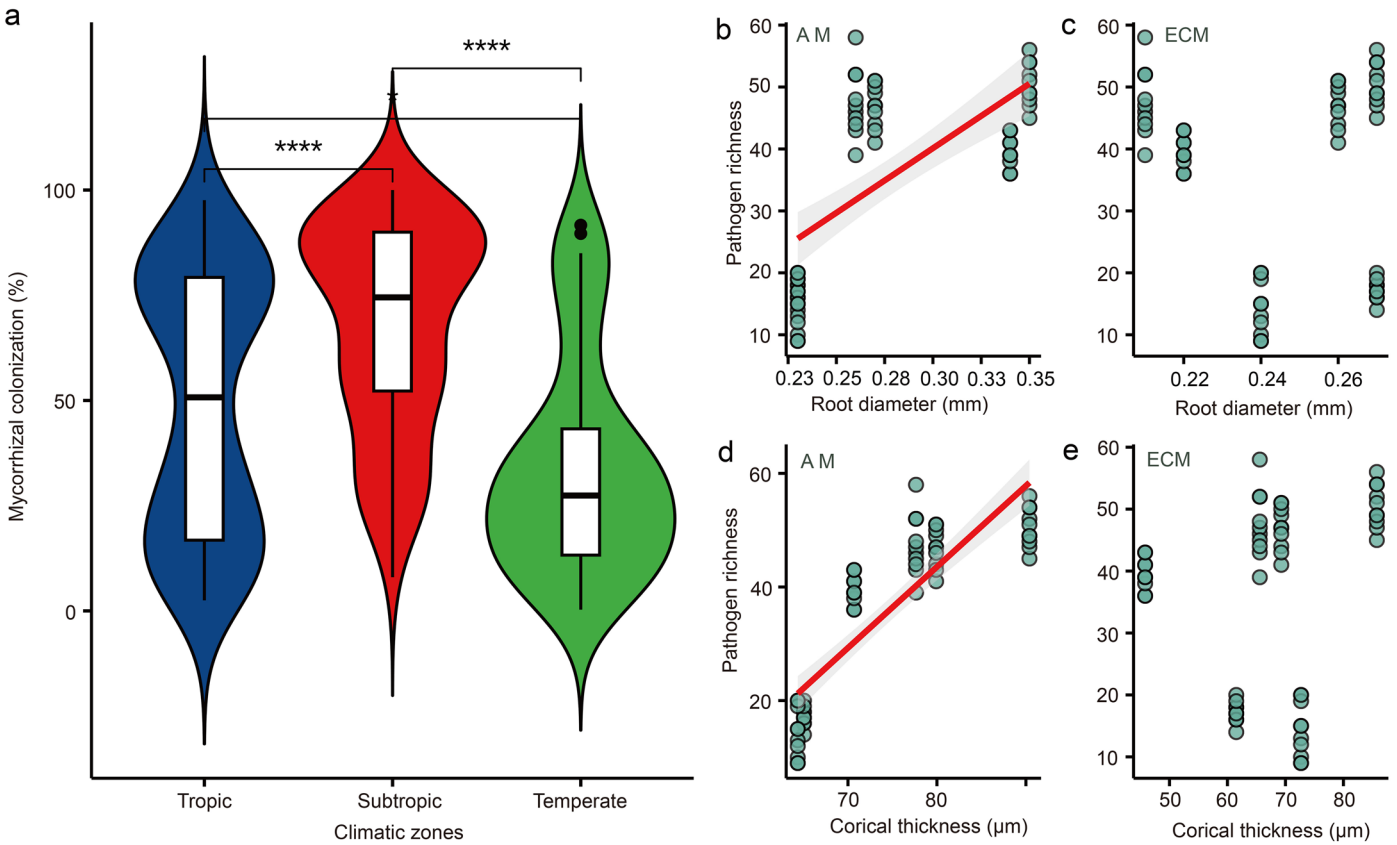

Extended Data Fig. 8 | Indirect evidence supporting the Pathogen Resistance Hypothesis. Analyses were performed using field-measured data of this study and literature data. **a**, there are differences in arbuscular mycorrhizal (AM) colonization rates across different climatic zones, with colonization rates in the tropics (blue) and subtropics (red) being higher than colonization rates in the temperate zone (green) ($n = 237$; *** $P < 0.001$). Pearson correlation indicates a positive correlation between soil pathogen richness and both root diameter and cortical thickness in arbuscular mycorrhizal (AM) plant species (**b**, $y = 208.43x - 22.41$, $r = 0.67$, $P = 6.59 \times 10^{-9}$; **d**, $y = 1.43x - 70.55$, $r = 0.85$, $P = 2.2 \times 10^{-16}$), but not in ectomycorrhizal (ECM) plant species (**c**, $r = 0.14$, $P = 0.25$; **e**, $r = 0.17$, $P = 0.20$). Shaded areas indicates 95% confidence intervals of the regression lines. The soil pathogen richness here were obtained through sequencing of soil samples collected from XSBN, DHS, SNJ, JGS, CBS, HZ sites (see the Methods section for details of these sites). The arbuscular mycorrhizal colonization data were collected from the GRooT database. Violin plots indicate the median value (solid line), the 25th and 75th percentiles (box), and the density of the data (width of the violin).

https://doi.org/10.1038/s41477-025-02089-4

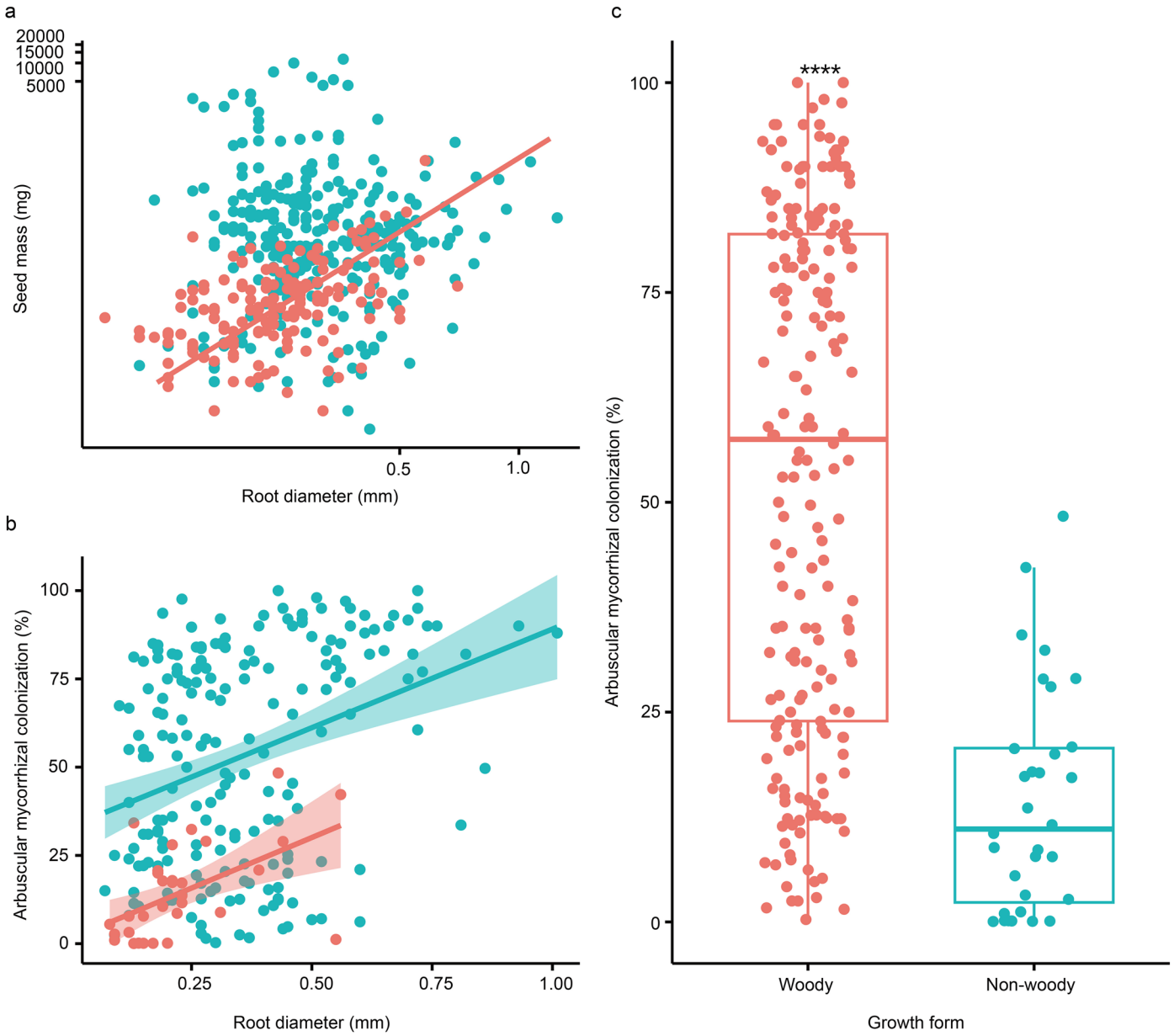

Extended Data Fig. 9 | Relationships between arbuscular mycorrhizal colonization rates and root diameter in woody and non-woody plants. Analyses were performed using field-measured data (**a**), as well as data from GRooT and literature (**b**, **c**). **a**, root diameter is positively related with seed mass in temperate non-woody species using the standardized major axis (SMA) regression (non-woody; **a**, $\log10(y) = 3.94 \log10(x) + 1.01$, $r = 0.46$, $P = 2.55 \times 10\text{-}11$, 95% CI = 3.46–4.50, $n = 285$), but not in temperate woody species (woody, a, $r = 0.06$, $P = 0.32$, $n = 284$). **b**, Pearson correlation indicates a significantly positive relationship between arbuscular mycorrhizal (AM) colonization and root diameter in both woody and non-woody plants (woody, $y = 55.88x + 33.25$, $r = 0.34$, $P = 9.66 \times 10\text{-}7$, $n = 202$; non-woody, $y = 57.24x + 1.44$, $r = 0.53$, $P = 0.001$, $n = 32$). Shaded areas indicates 95% confidence intervals of the regression lines. Mixed linear model showed no effect of plant growth form (woody versus non-woody) on the linear regression between arbuscular mycorrhizal colonization and root diameter ($P = 0.51$). **c**, boxplots of AM colonization rates by plant growth form; the red points represent woody plants, and the blue points represent non-woody plants. Horizontal lines in the middle of the box plots are the median AM colonization rates. There is a difference in AM colonization rate between woody and non-woody plants ($n = 234$, $P = 0.003$, $F = 50.57^{****}$). Each point representing one species. Box plots indicate the median value (solid line), 25th and 75th percentiles (box), and the data range (whiskers).

https://doi.org/10.1038/s41477-025-02089-4

Extended Data Table 1 | Summary of sampling information for all Chinese field sites where root traits were measured

Sampling site	*n*	Coordinates	MAT	Altitude	Tree	Shrub	Climatic zones
Xishuangbanna (XSBN)	235	21°10′-22°40′ N, 99°55′-101°50′ E	22.44	1000 (m)	163	72	Tropic
Dinghu Mountain (DHS)	93	23°09′-23°11′ N, 112°30′-112°33′ E	23.45	900 (m)	65	28	Subtropic
Jiulian Mountain (JLS)	28	24°31′-24°39′ N, 114°27′-114°29′ E	16.4	700 (m)	18	10	Subtropic
Gutian Mountain (GTS)	25	29°10′-29°17′ N, 118°03′-118°11′ E	19.38	850 (m)	11	14	Subtropic
Shennongjia (SNJ)	68	31°21′-31°36′ N, 110°03′-110°33′ E	15.89	1786(m)	39	29	Subtropic
Jigong Mountain (JGS)	33	31°46′-31°52′ N, 114°01′-114°06′ E	15.2	700 (m)	23	10	Subtropic
Taibai Mountain (TBS)	98	33°49′-34°05′ N, 107°22′-107°51′ E	13.66	2150 (m)	51	47	Temperate
Dongling Mountain (DLS)	18	39°55′-40°05′ N, 115°20′-115°35′ E	6.5	1200 (m)	5	13	Temperate
Liangshui (LS)	7	47°6″-47°16′ N, 128°47′-128°57′ E	2.72	650 (m)	5	2	Temperate
Changbai Mountain (CBS)	49	41°41′-42°25′ N, 127°42′-128°16′ E	6.84	900 (m)	25	24	Temperate
Huzhong (HZ)	6	51°17′-51°56′ N, 122°42′-123°18′ E	-0.16	800(m)	4	2	Temperate

Sampling site, (...) site abbreviation. n, number of species analysed. Coordinates, longitude and latitude. MAT, mean annual temperate. Tree, number of tree species. Shrub, number of shrub species.

nature portfolio

Corresponding author(s): Deling Kong, Guoyong Li, Junjian Wang

Last updated by author(s): Nov 1, 2024

Reporting Summary

Nature Portfolio wishes to improve the reproducibility of the work that we publish. This form provides structure for consistency and transparency in reporting. For further information on Nature Portfolio policies, see our Editorial Policies and the Editorial Policy Checklist.

Statistics

For all statistical analyses, confirm that the following items are present in the figure legend, table legend, main text, or Methods section.

n/a	Confirmed	
☐	☒	The exact sample size (*n*) for each experimental group/condition, given as a discrete number and unit of measurement
☐	☒	A statement on whether measurements were taken from distinct samples or whether the same sample was measured repeatedly
☐	☒	The statistical test(s) used AND whether they are one- or two-sided *Only common tests should be described solely by name; describe more complex techniques in the Methods section.*
☐	☒	A description of all covariates tested
☐	☒	A description of any assumptions or corrections, such as tests of normality and adjustment for multiple comparisons
☐	☒	A full description of the statistical parameters including central tendency (e.g. means) or other basic estimates (e.g. regression coefficient) AND variation (e.g. standard deviation) or associated estimates of uncertainty (e.g. confidence intervals)
☐	☒	For null hypothesis testing, the test statistic (e.g. *F*, *t*, *r*) with confidence intervals, effect sizes, degrees of freedom and *P* value noted *Give P values as exact values whenever suitable.*
☒	☐	For Bayesian analysis, information on the choice of priors and Markov chain Monte Carlo settings
☒	☐	For hierarchical and complex designs, identification of the appropriate level for tests and full reporting of outcomes
☐	☒	Estimates of effect sizes (e.g. Cohen's *d*, Pearson's *r*), indicating how they were calculated

Our web collection on statistics for biologists contains articles on many of the points above.

Software and code

Policy information about availability of computer code

Data collection	Data collection was conducted in two parts: 1. Field Sampling: Field - measured data were obtained by collecting samples from representative forest ecosystems in China, including 1 site in the tropical zone, 5 sites in the subtropical zone, and 5 sites in the temperate zone. 2. Database and Literature Review: Data were collected from the following sources: Global Root Trait (GRooT) Database (https://groot-database.github.io/GRooT/) TRY Plant Trait Database (https://www.try-db.org/TryWeb/Home.php) FungalRoot Database (Taxon occurrence data) (https://www.gbif.org/dataset/744edc21-8dd2-474e-8a0b-b8c3d56a3c2d) Relevant literature
Data analysis	We performed data analyses using some common packages in R-software (v.4.3.2), e.g. smart, U.PhyloMaker, Picante, caper, factoextra, funspace, phytools.

For manuscripts utilizing custom algorithms or software that are central to the research but not yet described in published literature, software must be made available to editors and reviewers. We strongly encourage code deposition in a community repository (e.g. GitHub). See the Nature Portfolio guidelines for submitting code & software for further information.

Data

Policy information about availability of data

All manuscripts must include a data availability statement. This statement should provide the following information, where applicable:

- Accession codes, unique identifiers, or web links for publicly available datasets
- A description of any restrictions on data availability
- For clinical datasets or third party data, please ensure that the statement adheres to our policy

The data of this study are available on Figshare (https://doi.org/10.6084/m9.figshare.28300658).

Research involving human participants, their data, or biological material

Policy information about studies with human participants or human data. See also policy information about sex, gender (identity/presentation), and sexual orientation and race, ethnicity and racism.

Reporting on sex and gender	Not applicable.
Reporting on race, ethnicity, or other socially relevant groupings	Not applicable.
Population characteristics	Not applicable.
Recruitment	Not applicable.
Ethics oversight	Not applicable.

Note that full information on the approval of the study protocol must also be provided in the manuscript.

Field-specific reporting

Please select the one below that is the best fit for your research. If you are not sure, read the appropriate sections before making your selection.

☐ Life sciences ☐ Behavioural & social sciences ☒ Ecological, evolutionary & environmental sciences

For a reference copy of the document with all sections, see nature.com/documents/nr-reporting-summary-flat.pdf

Ecological, evolutionary & environmental sciences study design

All studies must disclose on these points even when the disclosure is negative.

Study description	This study investigates the relationship between plant roots and seeds on a global scale and finds that mycorrhizal associations drive global coordination between roots and seeds.
Research sample	The global dataset (our field-measured data plus those from GRoot database and literature, 1280 species) includes 239 plant families and spans two major mycorrhizal types (1023 arbuscular mycorrhizal plants and 142 ectomycorrhizal plants), three growth forms (331 herbs, 329 shrubs, and 636 trees), and diverse climatic zones (380 tropical plants, 450 subtropical plants, and 467 temperate plants).
Sampling strategy	For each plant species, more than three mature individuals were selected, and more than 50 mature fruits or seeds were collected from each plant individual, the number depending on how many fruits or seeds matured in the individual plant. For small-sized seeds, more than 100 seeds per plant species were collected. We also collected at least 30 intact and undamaged leaves from the upper canopy . For the root , we traced the lateral roots starting from the main root of each tree and selected branches that contained at least five root orders. For each species, 15-20 first-order roots were selected from the FAA solution for anatomical analysis.
Data collection	we collected samples of roots, stems, leaves, and seeds from 660 woody plant species across 11 forest types in China, spanning climates from tropical to temperate regions. we also compiled data from the Global Root Traits (GRoot) database and other literature, incorporating 620 additional species with both root and seed traits data.
Timing and spatial scale	We collected species samples from 11 sites along a latitudinal gradient from southern to northern China, including 1 site in the tropical zone, 5 sites in the subtropical zone, and 5 sites in the temperate zone.
Data exclusions	No data were excluded.

Reproducibility

No data were excluded.

Randomization

Plant species were randomly selected according to the rules in "Research sample".
Plant individuals were randomly selected in the study site.
Samples were randomly selected in one tree.

Blinding

Blinding was not relevant to this study because this study mainly focused on the trait relationship rather than species variation.

Did the study involve field work? ☒ Yes ☐ No

Field work, collection and transport

Field conditions

Tropical Region
Xishuangbanna Tropical Rainforest Nature Reserve (101.25E, 21.95N) is located in the southern part of Yunnan Province, in the Xishuangbanna Dai Autonomous Prefecture. It is the only well - preserved tropical rainforest area in China. The reserve covers an area of approximately 2,420.2 square kilometers and includes various forest types such as tropical rainforests and evergreen broad - leaved forests. Xishuangbanna is situated south of the Tropic of Cancer and has a tropical monsoon climate with an average annual temperature of 22.5°C and an annual precipitation of 1,428 millimeters, characterized by year - round warmth and humidity.
Subtropical Region
Dinghushan National Nature Reserve (112.31E, 23.10N) is located in the central part of Guangdong Province. It is the first national nature reserve in China. The reserve is situated in the transitional zone between tropical and subtropical climates, with an annual rainfall of 1,900 millimeters and an average annual temperature of 20.9°C. Studies have shown that monsoon evergreen broad - leaved forests, mixed conifer - and - broadleaved forests, and Masson pine forests are the three representative main vegetation types in Dinghushan.
Jiulianshan National Forest Park (114.27E, 24.39N) is located on the north slope of Jiulianshan in the southwestern part of Longnan City, Jiangxi Province, at the core area of the Nanling Mountains on the border of Jiangxi and Guangdong provinces. It is situated in the transitional zone between the subtropical humid evergreen broad - leaved forests and the tropical monsoon evergreen broad - leaved forests. The park is a typical area in the eastern subtropical region with a well - preserved forest ecosystem. The annual rainfall is 2,155.6 millimeters, and the average annual temperature is 16.4°C.
Gutianshan Qianjiangyuan National Forest Park (118.03E, 29.17N) is located in the northwestern part of Kaihua County, Zhejiang Province. It is in the subtropical monsoon climate zone, with an annual rainfall of 2,100 millimeters and an average annual temperature of 16°C. The main vegetation types include mid - subtropical low - altitude primary evergreen broad - leaved forests, mixed evergreen and deciduous broad - leaved forests, mixed conifer - and - broadleaved forests, coniferous forests, etc.
Shennongjia National Nature Reserve (109.56E, 31.57N) is located in the northwestern part of Hubei Province. It is a transitional zone between subtropical and temperate climates, with an annual rainfall of 2,500 millimeters and an average annual temperature of 12° C. Shennongjia has the most complete vegetation vertical belt spectrum in the Northern Hemisphere. From low to high altitudes, the vegetation types are evergreen broad - leaved forest belt, mixed evergreen and deciduous broad - leaved forest belt, deciduous broad - leaved forest belt, mixed conifer - and - broadleaved forest belt, coniferous forest belt, and subalpine shrub and meadow zones.
Jigong Mountain National Nature Reserve (114.01E, 31.46N) is located in the southern part of Xinyang City, Henan Province. Jigong Mountain is a transitional climate zone between the northern subtropical humid and warm temperate semi - humid climates, which is the natural climatic boundary between the north and south of China. The average annual temperature is 15.2°C, and the average annual precipitation is 1,118.7 millimeters. The main vegetation types are evergreen coniferous forests, deciduous coniferous forests, mixed conifer - and - broadleaved forests, evergreen broad - leaved forests, and deciduous broad - leaved forests.
Temperate Region
Taibai Mountain (107.15E, 33.41N) is located at the junction of Taibai County, Meixian County, and Zhouzhi County in Shaanxi Province. It has typical subalpine climatic characteristics with distinct vertical climatic changes. The average annual temperature is 13°C, and the annual rainfall is 800 millimeters. The vegetation shows clear vertical zonation, with the vegetation types from low to high altitudes being the Quercus variabilis forest belt, the Betula forest belt, the coniferous forest belt, and the alpine shrub and meadow belt.
Donglingshan (115.20E, 39.55N) is located in Mentougou District, Beijing, and is part of the Taihang Mountains. The area has a temperate continental monsoon climate with mountainous climatic characteristics. The average annual temperature is about 6.5°C, and the annual precipitation is about 600 millimeters. The vegetation shows distinct vertical distribution characteristics with altitude changes. Deciduous broad - leaved forests are the zonal vegetation of this region.
Liangshui National Nature Reserve (128.47E, 47.16N) is located in the southeastern part of the Lesser Khingan Range. It has distinct temperate continental monsoon climatic characteristics. The annual rainfall is 676 millimeters, and the average annual temperature is 3°C. The vegetation types in the area include cold - temperate coniferous forests, temperate mixed conifer - and - broadleaved forests, deciduous broad - leaved forests, shrubs, meadows, and marshes.
Changbaishan (127.55E, 41.55N) is located in the southeastern part of Jilin Province, China. It has a temperate continental mountain climate. The annual rainfall is 700 millimeters, and the average annual temperature is 3°C. From the foot to the top of the mountain, the vegetation types are broad - leaved forests, mixed conifer - and - broadleaved forests, coniferous forests, alpine shrubs, and meadows.
Huzhong National Forest Park (122.53E, 52.11N) is located on the north slope of the Yilehuli Mountains in the northern section of the Greater Khingan Range. It has a cold - temperate continental monsoon climate. The annual rainfall is 497.7 millimeters, and the average annual temperature is as low as - 4.3°C. The main vegetation type is the cold - temperate coniferous forest.

Location

Xishuangbanna Tropical Rainforest Nature Reserve (101.25E, 21.95N) is located in the southern part of Yunnan Province, in the Xishuangbanna Dai Autonomous Prefecture. Dinghushan National Nature Reserve (112.31E, 23.10N) is located in the central part of Guangdong Province. Jiulianshan National Forest Park (114.27E, 24.39N) is located on the north slope of Jiulianshan in the southwestern part of Longnan City, Jiangxi Province. Gutianshan Qianjiangyuan National Forest Park (118.03E, 29.17N) is located in the northwestern part of Kaihua County, Zhejiang Province. Shennongjia National Nature Reserve (109.56E, 31.57N) is located in the northwestern part of Hubei Province. Jigong Mountain National Nature Reserve (114.01E, 31.46N) is located in the southern part of

	Xinyang City, Henan Province. Taibai Mountain (107.15E, 33.41N) is located at the junction of Taibai County, Meixian County, and Zhouzhi County in Shaanxi Province. Donglingshan (115.20E, 39.55N) is located in Mentougou District, Beijing, and is part of the Taihang Mountains. Liangshui National Nature Reserve (128.47E, 47.16N) is located in the southeastern part of the Lesser Khingan Range. Changbaishan (127.55E, 41.55N) is located in the southeastern part of Jilin Province, China. Huzhong National Forest Park (122.53E, 52.11N) is located on the north slope of the Yilehuli Mountains in the northern section of the Greater Khingan Range.
Access & import/export	Individual authors that contribute data determined the access to the study site.
Disturbance	Sampling activities of this study was conducted under the supervision of staff in the reserve. Therefore, no disturbance was caused by the study.

Reporting for specific materials, systems and methods

We require information from authors about some types of materials, experimental systems and methods used in many studies. Here, indicate whether each material, system or method listed is relevant to your study. If you are not sure if a list item applies to your research, read the appropriate section before selecting a response.

Materials & experimental systems

n/a	Involved in the study
☒	☐ Antibodies
☒	☐ Eukaryotic cell lines
☒	☐ Palaeontology and archaeology
☒	☐ Animals and other organisms
☒	☐ Clinical data
☒	☐ Dual use research of concern
☐	☒ Plants

Methods

n/a	Involved in the study
☒	☐ ChIP-seq
☒	☐ Flow cytometry
☒	☐ MRI-based neuroimaging

Dual use research of concern

Policy information about dual use research of concern

Hazards

Could the accidental, deliberate or reckless misuse of agents or technologies generated in the work, or the application of information presented in the manuscript, pose a threat to:

No	Yes	
☒	☐	Public health
☒	☐	National security
☒	☐	Crops and/or livestock
☒	☐	Ecosystems
☒	☐	Any other significant area

Experiments of concern

Does the work involve any of these experiments of concern:

No	Yes	
☒	☐	Demonstrate how to render a vaccine ineffective
☒	☐	Confer resistance to therapeutically useful antibiotics or antiviral agents
☒	☐	Enhance the virulence of a pathogen or render a nonpathogen virulent
☒	☐	Increase transmissibility of a pathogen
☒	☐	Alter the host range of a pathogen
☒	☐	Enable evasion of diagnostic/detection modalities
☒	☐	Enable the weaponization of a biological agent or toxin
☒	☐	Any other potentially harmful combination of experiments and agents

Plants

Seed stocks

The sources of samples in this study were obtained through the following means:
1. Collected through field.
2. Acquired through database and literature searches.
3. For species that could not be collected, seeds were obtained from the Germplasm Bank of Wild Species in Southwest China.

Novel plant genotypes

Not applicable

Authentication

In this study, the measured data were obtained through field sampling of species at 11 sampling sites.